

Grid Connected Modular Inverter with Fuzzy Logic Control for an Integrated Bidirectional Charging Station for Residential Applications

BDV MANIKANTA¹, Dr. M GOPICHAND NAIK²

^{1,2} *Department of Electrical Engineering, Andhra University College of Engineering, Visakhapatnam, Andhra Pradesh, India*

Abstract—This research work introduces a novel grid-connected modular inverter for an integrated bidirectional charging station (IBCS) primarily intended for residential and small-scale community energy systems. The proposed system is developed to meet the emerging demand for intelligent energy conversion interfaces that can effectively support electric vehicle (EV) charging, grid stability, and renewable energy management within the framework of a smart grid environment. The growing penetration of EVs and distributed renewable energy sources, such as solar photovoltaic (PV) and small wind turbines, has created new challenges in power balancing, grid stability, and energy utilization efficiency. This research aims to address these issues by proposing efficient, flexible, and intelligent inverter architecture capable of performing multiple functions in a residential setup.

The core of the proposed system is a modular bidirectional inverter that can operate seamlessly in several modes according to real-time grid conditions and user requirements. It functions both as an EV charger and as an energy interface between the EV battery, household loads, and the electrical grid. The system is designed to operate in bidirectional power flow mode—charging the EV battery from the grid or renewable energy sources when surplus power is available and discharging the battery to supply energy back to the grid or home loads during peak demand or outages. This bidirectional energy transfer capability makes the system suitable for Vehicle-to-Grid (V2G), Vehicle-to-Home (V2H) operations, thus extending its utility beyond simple charging infrastructure.

One of the key contributions of this work is the implementation of an advanced control strategy that enables efficient coordination among multiple energy sources. The proposed control approach is based on a low-level control strategy incorporating droop control and feedforward decoupling mechanisms to maintain stable voltage and frequency across the system during

load and generation variations. The droop control technique, traditionally used in microgrid applications, is employed here to achieve decentralized power sharing and ensure smooth transitions between grid-connected and islanded operating modes.

To enhance the performance of conventional controllers, the system integrates a hybrid control scheme combining a Proportional-Integral (PI) controller with a Fuzzy Logic Controller (FLC). While the PI controller ensures steady-state accuracy, the fuzzy logic component improves adaptability and robustness under dynamic operating conditions. The FLC does not rely on an exact mathematical model of the system, allowing it to handle nonlinearities and parameter uncertainties effectively. This hybrid control structure enhances the system's dynamic response, minimizes overshoot and settling time, and ensures reliable operation under varying grid voltages, load disturbances, and temperature changes.

The system's overall functionality is comprehensively evaluated through detailed MATLAB/Simulink simulations, which model various real-world scenarios including grid-connected operation, standalone mode, and transitions between different power flow states. The simulation results validate the effectiveness of the proposed control algorithm in maintaining voltage and current stability, regulating power flow, and ensuring seamless mode transitions. The results also demonstrate the system's ability to support the grid during peak demand periods by discharging stored energy from the EV battery, thereby reducing stress on utility infrastructure and enhancing overall grid resilience.

I. INTRODUCTION AND LITERATURE REVIEW

1.1 Introduction

Concerns over pollution and resource depletion have increased the popularity of electric vehicles (EVs) [1]. The increasing demand for electric vehicles

necessitates the installation of charging stations. Electric vehicle batteries are normally charged by utility power. [2-4] present grid-based charger topologies for charging EV batteries. These topologies require large amounts of grid power to charge the EV batteries. On the other hand, the charger's unidirectional current flow architecture prevents the actual current from flowing backwards from the car to the grid. EV batteries can be used as a kind of energy storage to harness power when demand is high [5]. an overwhelming majority.

Most of the time, electric cars are parked with a large amount of energy stored. It's an electric car when not in use, the grid receives power from the battery to cover peak demand. To do this, the electric vehicle charger must allow bidirectional active power flow [6]. The way electric vehicles send power to the grid is known as "Vehicle to Grid" (V2G). In this mode, EV charging is capable of providing reactive power support to the grid [7-10]. Supports reactive power near the end of the load[9]. PV disruption is eliminated by using EV batteries as buffer storage and connecting charging stations to the grid[10, 11]. Demonstrated the effectiveness of on-board charging in charging EV batteries. Batteries with low power consumption, on the other hand, are charged on board. As such, off-board chargers are a more practical choice than on-board chargers. [12–13] Examine the off-board charger topology.

Current research envisions a single-stage, solar-powered, off-board charging station for grid-connected electric vehicles. This outlet allows power to flow in both directions. A bi-directional converter connects the electric vehicle to his DC intermediate circuit at the charging station. Bi-directional converters protect EV batteries from second harmonic currents and DC link ripple, extending battery life. Furthermore, the battery performance of electric vehicles is no longer determined by the intermediate circuit voltage. The bidirectional converter's duty cycle controls battery charging and discharging. PV arrays are used to charge electric vehicle (EV) batteries, sending additional power to the utility company, alleviating the need for generators.

The VSC provides the required reactive power regulation for the grid. Connecting solar-powered EV charging stations to the grid improves the quality of the grid power supply. It operates independently in

grid failure mode to generate power for the PV array and charge the EV batteries. The system is also evaluated under various dynamic conditions, such as: B. Fluctuations in photovoltaic solar radiation, grid voltage imbalance, and changes in reactive power in the grid. The charging station will sync with the network when restored. Active and reactive power reference instructions are used in the charging station control architecture. Electric vehicle owners use the reference active power command to determine whether to charge or discharge the electric vehicle battery.

The reference reactive power is selected according to the inductive/capacitive reactive power parameters required for continuous operation of the charging station. Charging stations are configured so that electric vehicle owners can choose their own charging and discharging times. System operation when mains power is needed to charge an EV battery, it is called G2V (Grid to Vehicle). The system is called V2G (Vehicle to Grid), in which the battery of an electric vehicle discharges to power the grid. Depending on the situation, the charging station can also adjust reactive power (delay/lead).

1.2 Literature Review

The increasing integration of electric vehicles (EVs) into residential applications necessitates the development of efficient and sustainable charging solutions. Existing research has explored various charging methodologies, particularly focusing on bidirectional charging stations that enable Vehicle-to-Grid (V2G) and Vehicle-to-Home (V2H) functionalities. The literature highlights the need for modular inverters to enhance energy management and grid stability while ensuring optimal power flow between the EV battery, household loads, and the power grid.

Bidirectional Charging and Energy Management

Bidirectional charging technology plays a crucial role in energy buffering and grid support. Several studies emphasize that EV batteries can store excess energy during low-demand periods and discharge it back to the grid during peak hours. This technology enhances energy utilization efficiency, reduces dependency on conventional energy sources, and provides a potential revenue stream for EV owners through grid energy resale [1]. The use of a modular inverter in bidirectional charging stations further improves

system reliability by allowing adaptive power flow management and voltage regulation [2].

Control Strategies for Smart Charging

Various control strategies have been proposed to manage energy exchange between EVs and the grid. The conventional proportional-integral (PI) controller is widely used in energy management systems; however, its limitations in dynamic adaptability necessitate alternative approaches. Recent studies indicate that replacing PI controllers with fuzzy logic controllers (FLC) improves system robustness and adaptability under varying grid conditions. FLC enables efficient energy distribution and enhances voltage stability by dynamically adjusting power flow parameters [3]. Additionally, droop control techniques and feedforward decoupling have been explored to optimize power flow and minimize disruptions in grid operations [4].

Renewable Energy Integration with EV Charging

The integration of Renewable Energy Sources (RES) with EV charging stations has gained significant attention. Solar photovoltaic (PV) systems are commonly used in residential energy setups, contributing to decentralized power generation. Research indicates that solar energy's share in power production is expected to increase from 33% to 67% by 2030, with a substantial portion coming from rooftop installations [5]. Combining RES with bidirectional charging infrastructure can further enhance sustainability by reducing reliance on grid electricity and enabling self-sufficient energy management [6].

Communication Protocols and System Interoperability

An essential aspect of bidirectional charging systems is the implementation of standardized communication protocols to ensure seamless operation. The ISO 15118-20 protocol facilitates secure and efficient data exchange between EVs and charging stations, allowing real-time energy flow management. Power Line Communication (PLC) has been identified as a viable method for extracting EV battery information and enabling smart charging operations [7]. Studies have also examined the CHAdeMO and Combo CCS Type 2 connectors for bidirectional energy transfer, highlighting their potential in enhancing the practicality of V2G and V2H applications [8].

Economic Feasibility and Cost Considerations

Economic assessments of DC charging infrastructure suggest that integrating bidirectional charging with residential energy management systems can significantly reduce the Total Cost of Ownership (TCO). Recent studies indicate that such systems can lead to a 30% reduction in operational costs for EV charging network operators while providing financial benefits to homeowners through reduced grid dependency and optimized energy consumption [9]. However, challenges such as infrastructure costs and policy limitations still need to be addressed to facilitate widespread adoption [10].

The reviewed literature underscores the importance of developing an efficient and adaptive bidirectional charging system for residential applications. Modular inverter technology, coupled with advanced control strategies such as fuzzy logic controllers and droop control techniques, enhances system performance and energy efficiency. Furthermore, integrating RES and implementing robust communication protocols can further optimize the functionality of V2G and V2H systems. Future research should focus on addressing infrastructure challenges and refining economic models to promote the large-scale deployment of sustainable EV charging solutions.

1.3 The Objective of the thesis

This project aims is to modeling, control and validation towards the integration of an EV charging station, Renewable Energy Sources with a grid interfacing inverter to buffer the Energy Source System (ESS) for residential applications. . This research tackles the bidirectional DC charging station which is not only able to charge the EV during off peak load times but can also utilize the RES to minimize the energy cost of the owner

1.3.1 This research introduces a new kind of EV charging station that helps:

- Charge an EV faster and more efficiently.
- Store excess energy from solar panels or the grid and use it when needed.
- Send power back to the grid (V2G) to balance electricity demand.
- Power a home using the EV battery (V2H) during blackouts.

1.3.2 This system enhances grid stability by providing buffering services and supporting energy management. To optimize power flow between the EV battery, household load, and the grid, a low-level

control strategy based on the droop control technique and feedforward decoupling is implemented, replacing the conventional PI controller with a fuzzy logic controller (FLC). The system's performance is evaluated through MATLAB/Simulink simulations, demonstrating its ability to support the grid during peak demand and enhance renewable energy integration.

1.3.3 Overall, this research work focus on development of sustainable and smart charging solutions for electric vehicles.

1.3.4

1.4 Organisation of the thesis: This thesis has been categorised into five chapters as outlined below: Chapter 1 – Introduction and Literature Review, Chapter 2 – DC Charging station integrated with grid connected inverter, Chapter 3 – Simulation of PV Systems, BEES, 3-φ Load and Grid, PWM, Chapter 4 – Control strategies for proposed integrated DC charger Inverter system, Chapter 5 – Results and Discussion, Chapter 6 – Conclusion and Future work

II. DC CHARGING STATION INTEGRATED WITH GRID CONNECTED INVERTER

2.1 Conventional power generation mix including EV charging and house load supply from Solar PV, BESS and grid

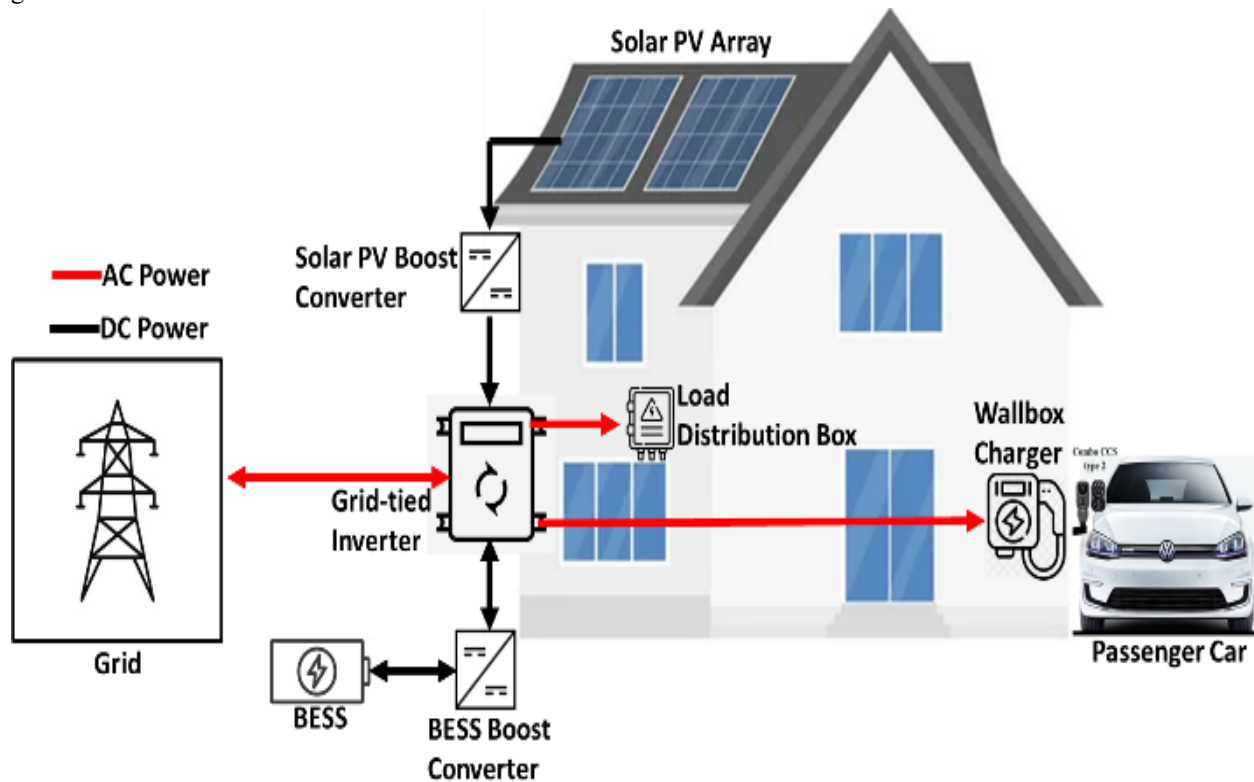


Fig 2.1 - Conventional power generation mix system for household application

A conventional power generation mix system for household applications is shown in Figure 2.1. The grid-tied inverter rated 10kW is the central component of this system as it supplies the DC power from 10 kWp Solar PV to the house load and electric vehicle charger wall box with AC power [18], [19]. The house load monthly consumption is considered

20 kWh which is an average electricity consumption for a 4-person family.

2.2 Proposed integrated DC charger with grid-connected inverter system

The power generation mix system architecture with integrated DC EV charger with grid-connected inverter integration is shown in Figure 2.2. The proposed system can enable bidirectional upto 22 kW

DC charging and V2G service at home via Combo CCS Type 2 charging port. Moreover, the system can use the EV battery as energy buffer for house load

during emergency condition and/or regular power backup in the evening. During hot summer

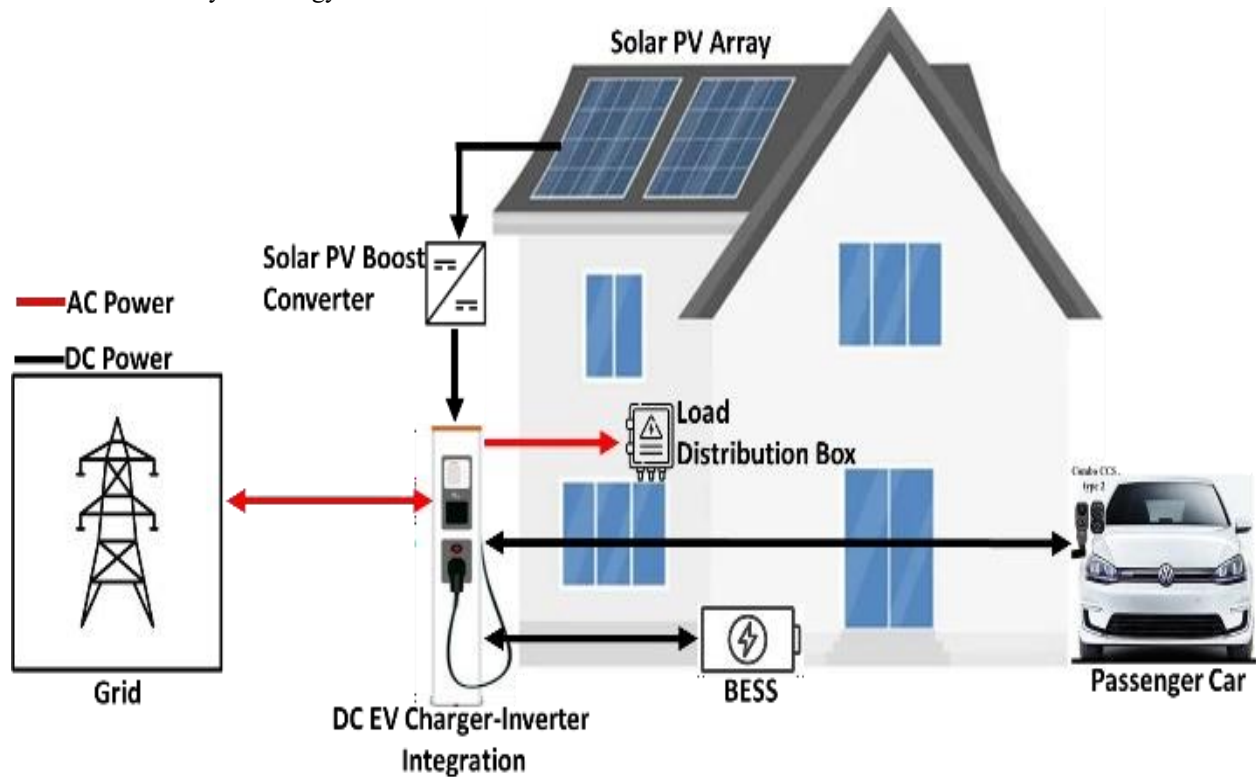


Fig 2.2 - Proposed integrated DC charger with grid connected inverter system including EV charging and house load supply from Solar PV, BESS and grid

days, the share of solar power in the energy mix is high and can be sufficient to cover the house load demand and send the surplus energy to the home BESS to charge it or send energy back to the grid if the BESS is fully charged. Using the proposed bidirectional charging station solution, the solar power from the PV system can also be stored in electric cars and home batteries during day time and

feedback into the home grid in the evening hours or when needed to operate household appliances. In this case, the size of the BESS can be reduced from standard battery sizing calculation or solar home system [18]. The novelty of this research work is summarized in Table 2.2 which illustrates the improvement scopes of the conventional system with proposed novel solution.

Table 2.2 - Improvement scope of the conventional system with proposed system

Improvement Scopes	Conventional System	Proposed System
AC Slow Charging	Yes	Yes
AC Fast Charging	No	Yes
DC Charging	No	Yes
V2G	No	Yes
V2H	No	Yes
Smart Charging	No	Yes
Charging Port	MennekesType2	ComboCCS2
Communication	OCPP2.0j	ISO15118.20
Charging Time	10.5 hour (7.4kW)	4 hour (22kW)

2.3. Operating modes of integrated DC charging station with grid connected inverter

2.3.1 EV Charging mode from grid:

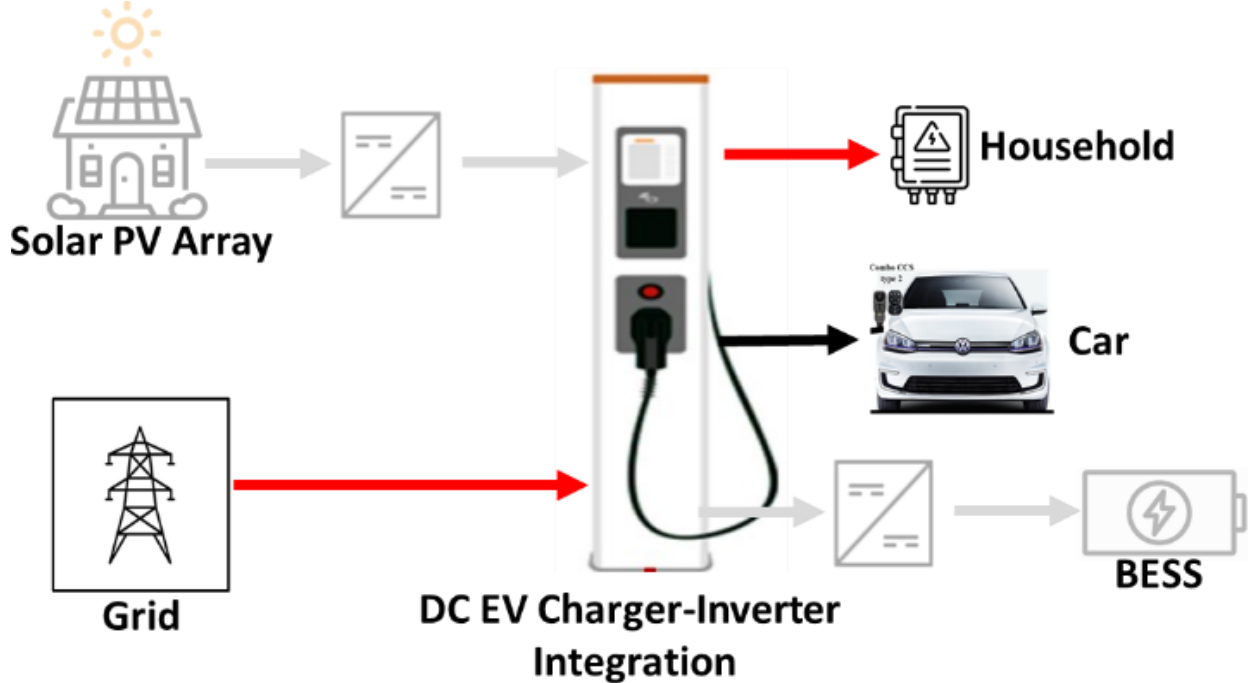


Fig 2.3.1 - EV Charging mode from grid

Since there is no solar generation during 0800 pm to 0500 am, the EV uses power from the grid to charge. The house load demand can also be fulfilled by grid.

2.3.2 Off-grid inverter mode:

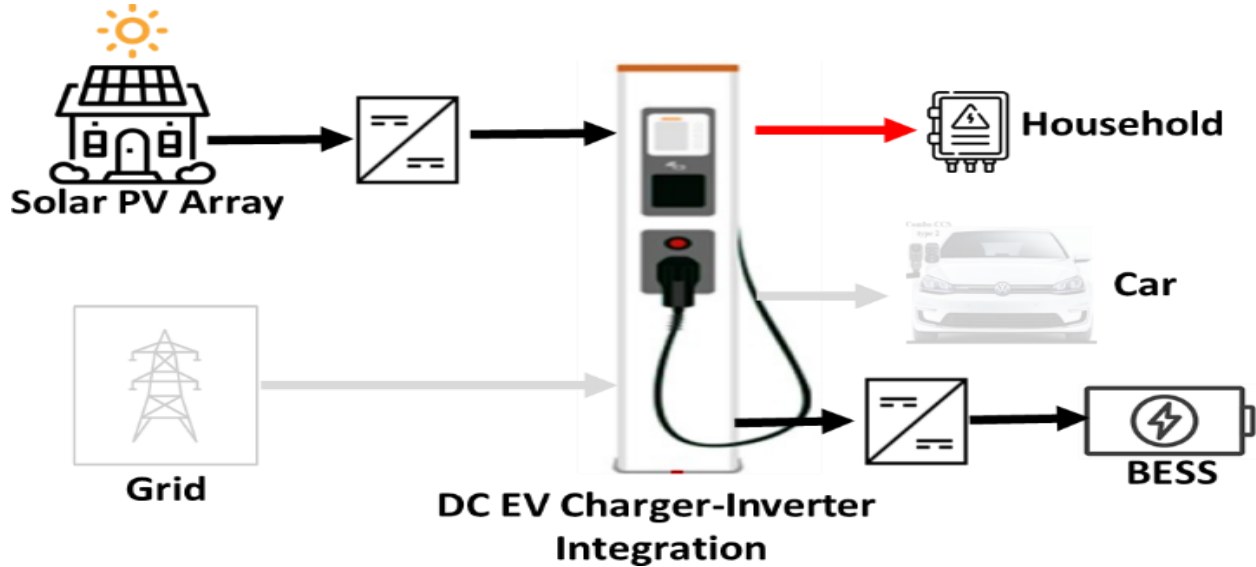


Fig 2.3.2 - Off-grid Inverter mode to supply the load from Solar PV

The solar irradiance provides energy during the peak time (7.00am-4.00pm) when the EV is off to the office with around 95% SoC. The integrated charging station works in off-grid inverter mode or islanding

mode to supply the household load and store the excess energy to the BESS system or send back to the grid.

2.3.3 V2H Mode:

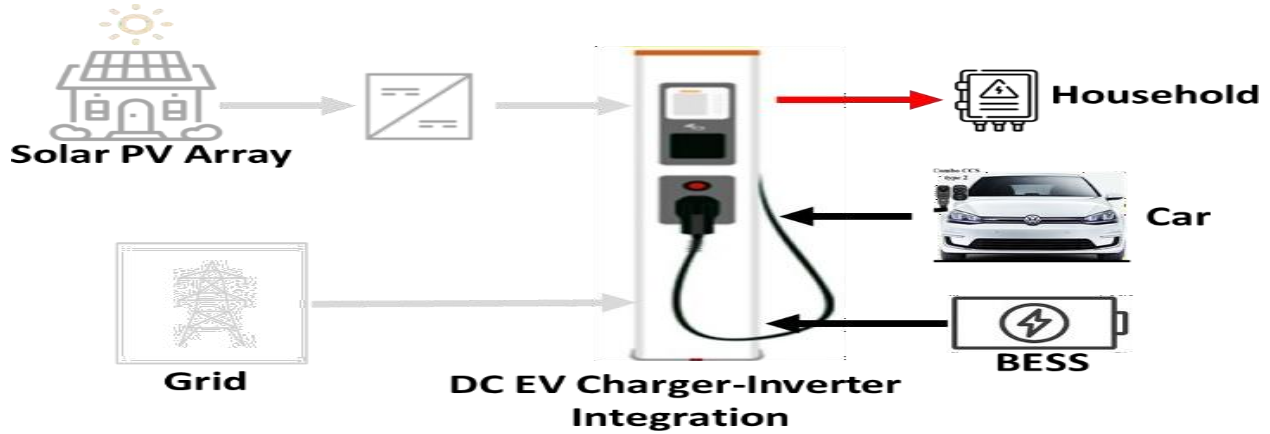


Fig 2.3.3 - V2H mode to supply the load from EV battery

The proposed system works as V2H mode during the evening (05.00pm-11.00pm) when the EV returns home with around 60% SoC. The required household load demand in the evening can be fulfilled by combining both the use of the EV battery storage and BESS.

2.3.4 V2G Mode:

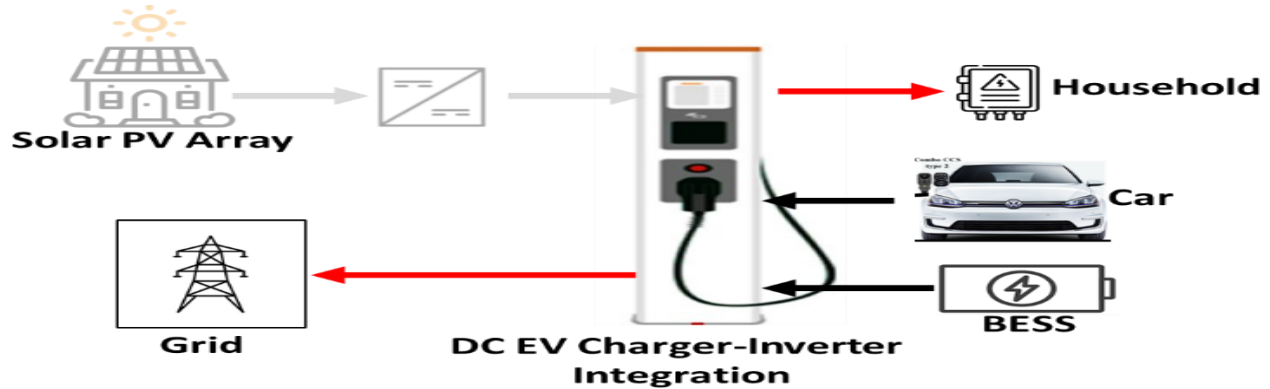


Fig 2.3.4 - V2G mode to transfer power back to the grid from EV battery

The V2G mode activation generally depends on the massive voltage and frequency fluctuation which requires the homeowner's consent. In this mode, the proposed system works as grid-connected mode to transfer the battery power to the grid. The household load can be supplied from the BESS.

2.4 Charging Methods: The research examines the constant current-constant voltage charging method based on the equivalent circuit model of the lithium-ion battery, together with the commonly used constant power-constant voltage (CP-CV) and constant current-constant voltage (CC-CV) methods. On top of that, we offer a loss-constant voltage charging method. The research compares and contrasts all of these different kinds of charges.

2.5 State-Space modeling of parallel grid connected DC/AC converter

Fig 2.5.1 illustrates a charging station that is composed of multiple AC/DC converter modules connected in parallel with LCL filter. Each filter has a damping resistor, R_d , connected to the filter capacitors, C_f . The model takes into consideration the converter-to-grid side and grid-to-converter side mutual coupling terms, M_{cg} and M_{gc} , of the three-phase converter-and grid-side inductors, L_c and L_g , respectively. It is important to note that these coupling terms are often neglected, even if three-phase inductors are used in place of one inductor per phase. It is necessary to consider the three-phase inductors due to the significant effect on the dynamic response of the system. The model also includes the grid inductance, L_s .

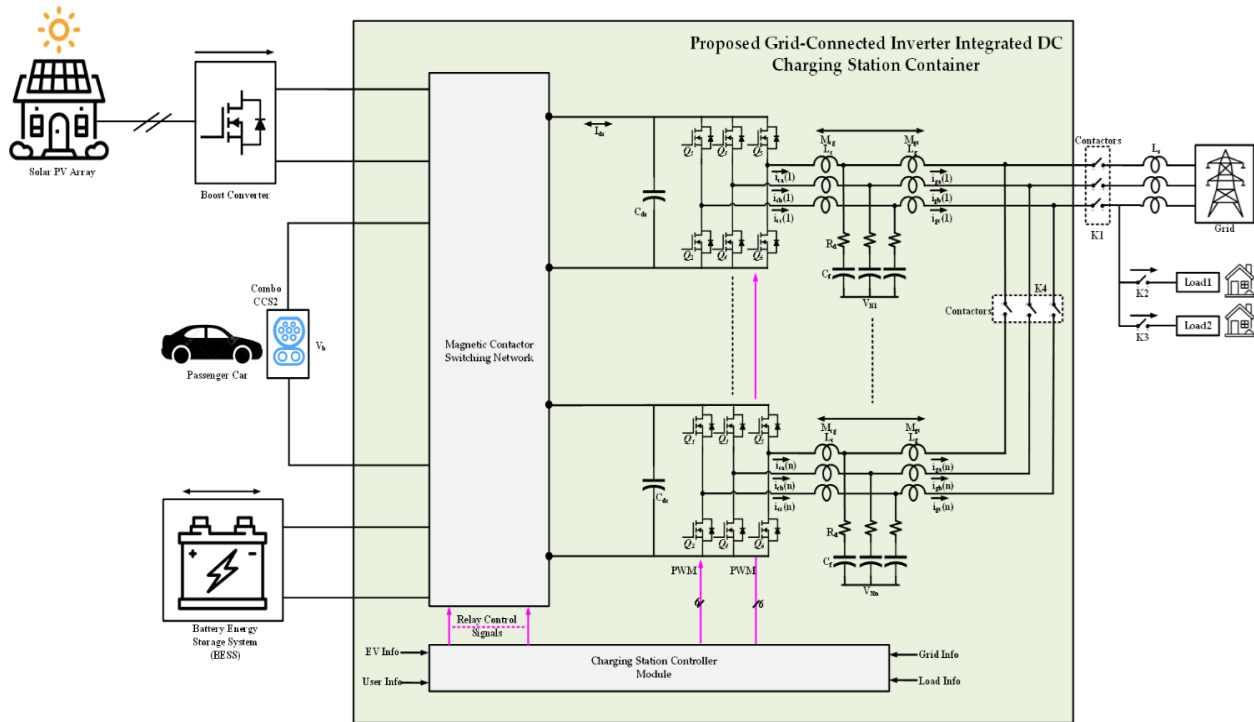


Fig 2.5.1 - Bi-directional AC/DC converter with LCL filter connected to grid and house load

The small signal equivalent circuit of each half-bridge module which is shown in Fig 2.6.2 can be used to derive an averaged model of the parallel V2G converters with n number module in the stationary three-phase frame, as demonstrated in Fig 2.6.3. The converter-side currents are denoted as I_{cx} , whereas I_{gx} represents the grid-side currents. The grid source

currents are expressed as I_{sx} . Note that x is the notation of three phases (a, b and c phase). Moreover, the duty cycle of three-phase leg in the synchronous reference frame denoted as S_a , S_b and S_c . The state space model of the n parallel V2G charger module comprises the state and input matrices.

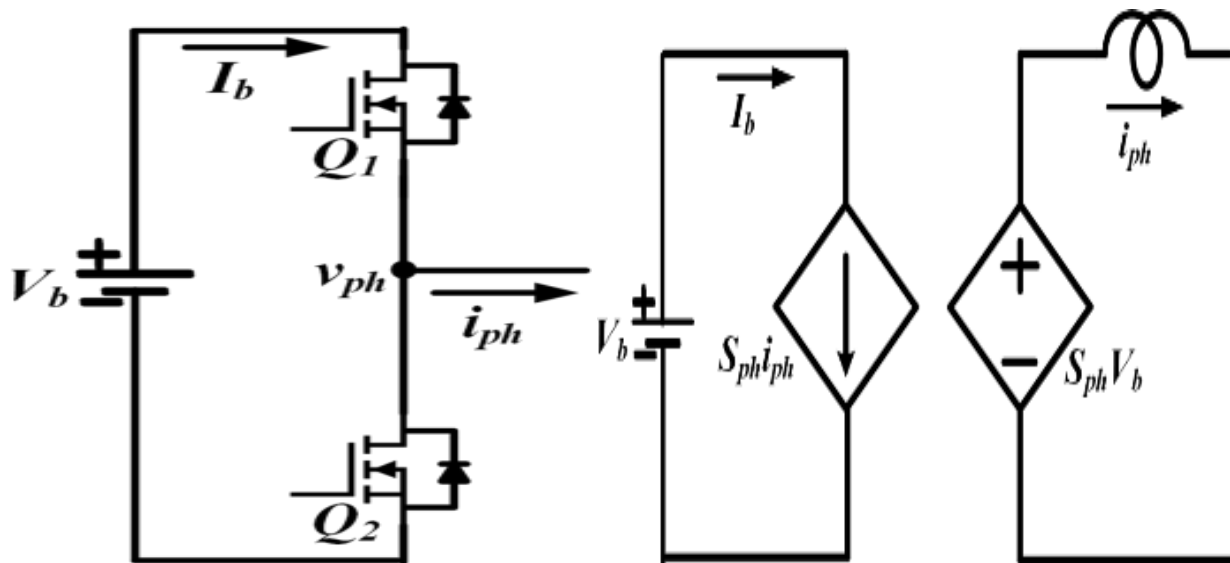


Fig 2.6.2 - Small signal average model for half bridge

However, two converters are considered for this project work. These matrices can be derived from the dynamic equation of each state variable of the system.

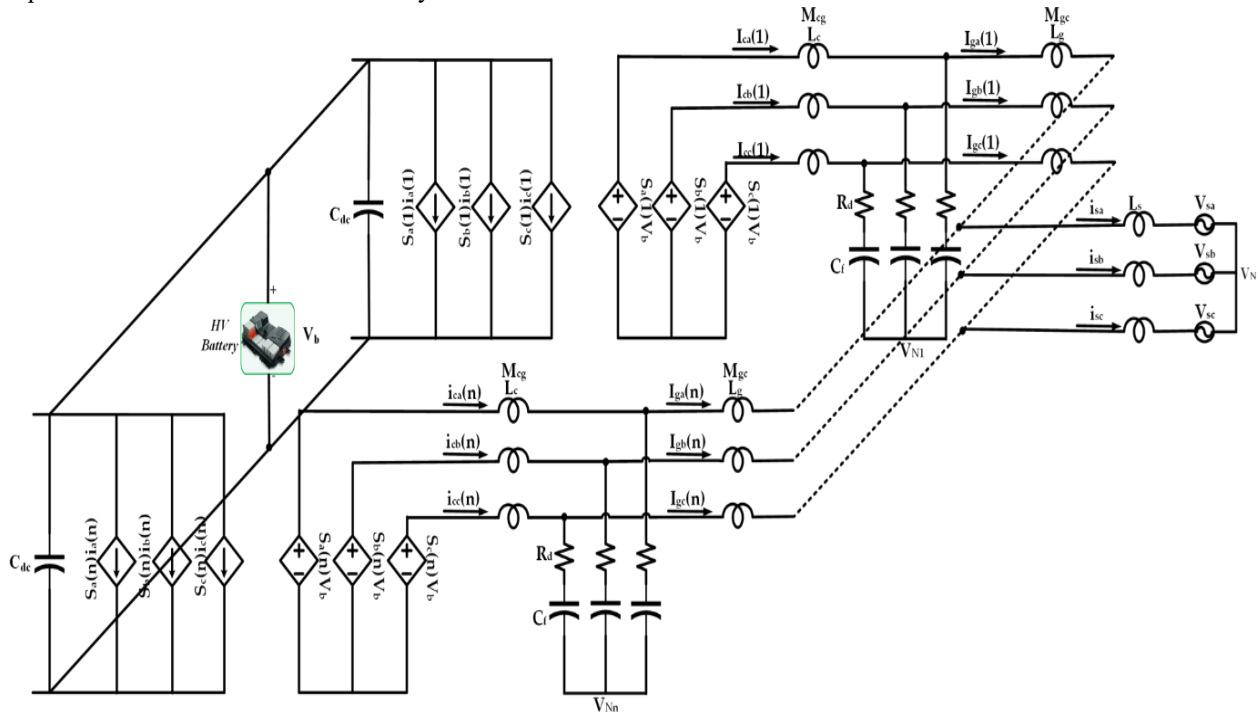


Fig 2.6.3 - Small signal average model of a parallel AC/DC converter module with LCL filter

In this system, the LCL filter is the main part for the dynamic performance of the system. Thus, the state variables of such a system are the inductor currents and the voltage across the filter capacitor. The state variables of n parallel V2G converter systems are expressed in (1) where the superscript “c” and “g” represent the converter and grid sides, respectively. Moreover, the superscript “f” denotes the filter. The input variables are the duty cycles in synchronous reference frame (SRF) which are expressed in (2). The state and input equations of the model in the SRF frame have been obtained from (3) where the input

vector U contains both control variables (the duty cycles of each inverter leg) and disturbances (the d and the q terms of the grid voltage). A, B, C and D are the auxiliary matrices which can be formulated from the dynamic equation of state variables. To derive the simplified dynamic equations, we can consider that the charger system has been configured utilizing an SRF, in which the grid voltage is aligned to the d -axis. This setup allows independent manipulation of the active power with the d -axis current, while the reactive power can be regulated with the q -axis current.

$$X = Y = [i_d^c(1), i_q^c(1), i_0^c(1), i_d^g(1), i_q^g(1), i_0^g(1) \dots i_d^c(n), i_q^c(n), i_0^c(n), i_d^g(n), i_q^g(n), i_0^g(n)] \quad (1)$$

$$\dots v_d^f(1), v_q^f(1), v_0^f(1) \dots v_d^f(n), v_q^f(n), v_0^f(n)]^T$$

$$U = [s_d(1), s_q(1), s_0(1) \dots s_d(n), s_q(n), s_0(n), v_d^g, v_q^g, v_0^g]^T \quad (2)$$

$$\frac{d}{dt}X = AX + BU \quad (3)$$

$$Y = CX + DU$$

To derive the simplified dynamic equations, we can consider that the charger system has been configured utilizing an SRF, in which the grid voltage is aligned to the d-axis. This setup allows independent manipulation of the active power, with the d-axis current, while the reactive power can be regulated with the q-axis current. The 0-axis current, which is the zero-sequence component, can also be adjusted to control the circulating current. The State equations are given at equation 4 to 6.

Here $[x_{dq0}^c(k)] = [i_d^c \ vq^c \ v0^c]^T$ represents the voltage and currents of the converter-side inductor, and $[x_{dq0}^g(k)] = [i_d^g \ vq^g \ v0^g]^T$ for the grid-side inductor. Similarly, $[V_{dq0}^f(k)] = [v_d^f \ vq^f \ v0^f]^T$ are expressing the voltage across the filter capacitor. The output voltage dynamic equation is shown in equation (7) where V_b and I_b represent the voltage and current of the

$$\frac{d}{dt} [x_{dq0}^c(k)] = -T \frac{dT^{-1}}{dt} [i_{dq0}^c(k)] + V_b I_{L1} [s_{dq0}(k)] - I_{L1} [v_{dq0}^f(k)] + R_d I_{L1} [i_{dq0}^c(k)] + R_d I_{L1} [i_{dq0}^g(k)] - \sqrt{3}(V_n' - V_n) I_{L1} \begin{bmatrix} 0 \\ 0 \\ 1 \end{bmatrix} \quad (4)$$

$$\frac{d}{dt} [x_{dq0}^g(k)] = -T \frac{dT^{-1}}{dt} [i_{dq0}^g(k)] + I_{L2} [v_{dq0}^c(k)] + R_d I_{L2} [x_{dq0}^c(k)] - R_d I_{L2} [i_{dq0}^g(k)] - I_{L2} [v_{dq0}^s(k)] - \sqrt{3}(V_n' - V_n) I_{L2} \begin{bmatrix} 0 \\ 0 \\ 1 \end{bmatrix} \quad (5)$$

$$\frac{d}{dt} [V_{dq0}^f(k)] = -T \frac{dT^{-1}}{dt} [i_{dq0}^g(k)] + \frac{1}{C_f} \{ [i_{dq0}^c(k)] - [i_{dq0}^g(k)] \} \quad (6)$$

$$\frac{d}{dt} V_b = \frac{1}{nC_{dc}} (I_b - [s_{dq0}(k)] * [i_{dq0}^c(k)]) \quad (7)$$

$$T = \sqrt{\frac{2}{3}} \begin{bmatrix} \cos \omega t & \cos \left(\omega t - \frac{2\pi}{3} \right) & \cos \left(\omega t + \frac{2\pi}{3} \right) \\ -\sin \omega t & -\sin \left(\omega t - \frac{2\pi}{3} \right) & -\sin \left(\omega t + \frac{2\pi}{3} \right) \\ \frac{1}{\sqrt{2}} & \frac{1}{\sqrt{2}} & \frac{1}{\sqrt{2}} \end{bmatrix} \quad (8)$$

$$T \frac{dT^{-1}}{dt} = \begin{bmatrix} 0 & -\omega & 0 \\ \omega & 0 & 0 \\ 0 & 0 & 0 \end{bmatrix} \quad (9)$$

battery. The conversion matrix, T expressed in (8) is used to convert the *abc* frame to *dq* frame comprised with grid angular frequency, \mathcal{G} . To simplify the dynamic equation, the T matrix is reformulated in terms of \mathcal{G} which is expressed in (9). In these equations, *k* indicates the converter identifications connected in parallel ($k = 1, 2, 3 \dots \dots n$). The auxiliary matrices, A, B, C and D are obtained after a detailed formulation of the above-mentioned dynamic equations.

III. SIMULINK IMPLEMENTATION OF PV SYSTEMS, EV, BESS, 3-Φ LOAD, GRID, PWM

3.1 PV System

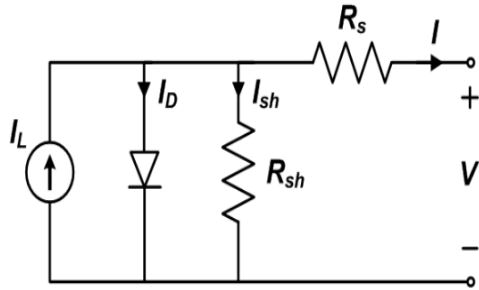
This section provides an overview of renewable energy sources and how to model them is given in this chapter. Before any renewable energy source is built, its design will be validated in MATLAB/Simulink. A photovoltaic cell, often called

a "solar battery," is a kind of electrical device that leverages the photovoltaic effect—a physical and chemical phenomenon—to directly transform the energy of light into electricity. Light may cause certain electrical characteristics, such as current, voltage, or resistance, to change in a device called a photoelectric cell. Photovoltaic modules, more often known as solar panels, are built around solar cells. Whether they use artificial light or sunshine, solar cells are always called photovoltaic. They measure

the intensity of light or detect light or other electromagnetic radiation near the visual range; examples of photo detectors include infrared detectors.

3.2 Equivalent Circuit of a Solar Cell

The electrical model shown in Figure 3.2.1 may serve as a representation of the solar cell. Here is the equation that represents its current voltage characteristic.



$$I = I_L - I_0 \left(e^{\frac{q(v-IR_s)}{AKT}} - 1 \right) - \frac{v-IR_s}{R_{sh}}$$

Fig 3.2.1 - Equivalent circuit of a solar cell

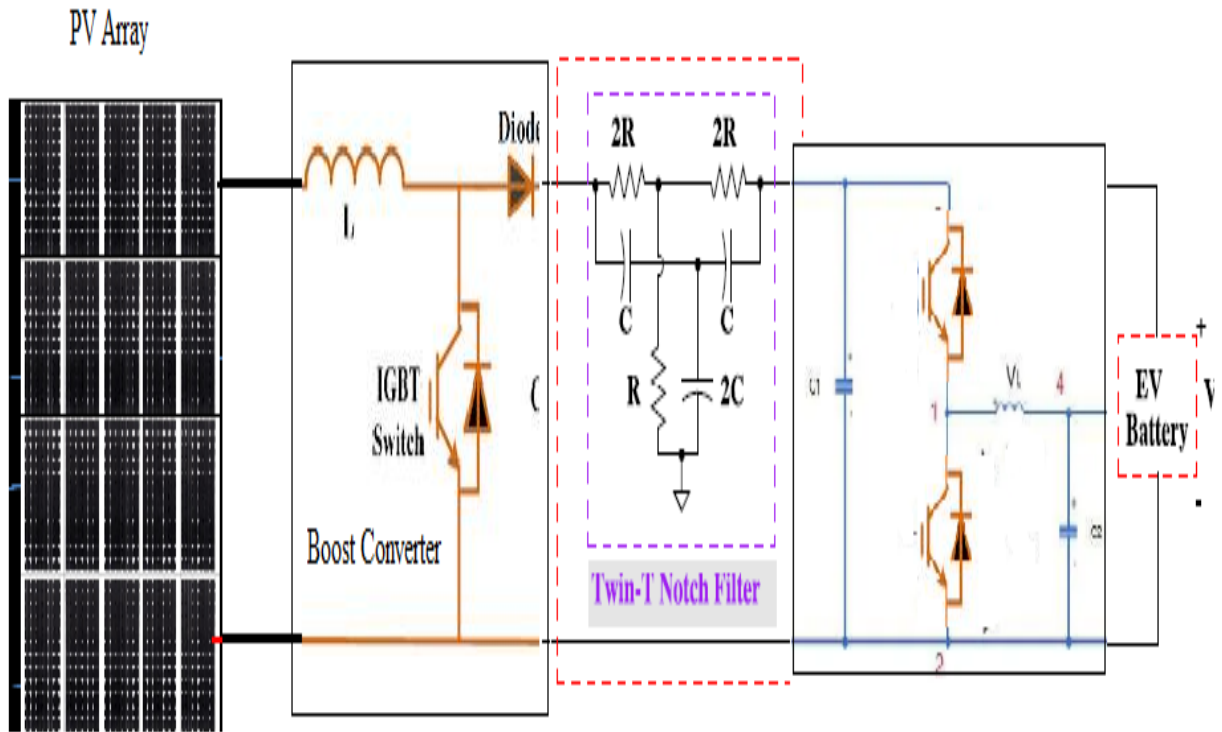


Fig 3.2.2 - PV system

3.5 Pulse Width Modulator

In order to regulate the on/off time ratio, you compare this with a d.c. voltage and tweak it as needed. Accumulating a triangle voltage greater than the 'demand' voltage causes the output to rise. Assuming the triangle's voltage is lower than the demand voltage, the

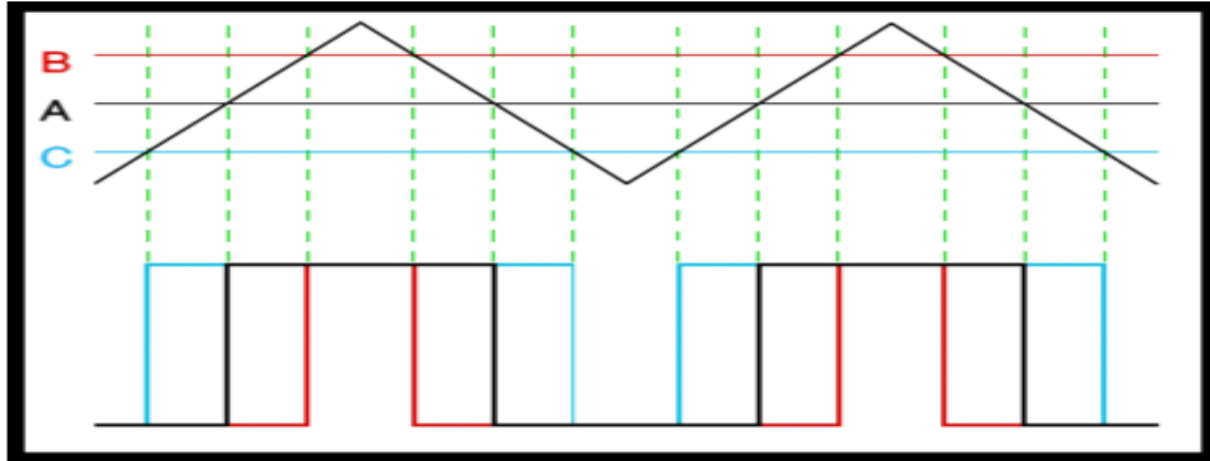


Fig 3.5.1 - Pulse reference representations

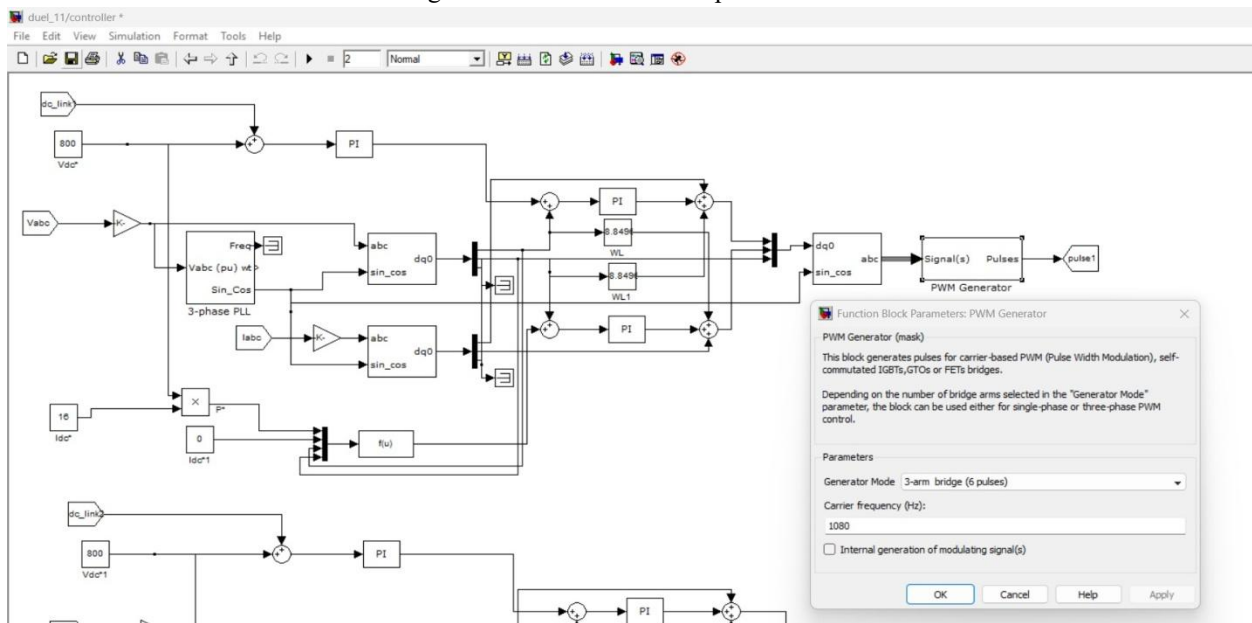


Fig 3.7.2 - Simulation diagram of PWM Generator

IV. CONTROL STRATEGIES FOR PROPOSED INTEGRATED DC CHARGER-INVERTER SYSTEM

4.1 Control strategies

The proposed bidirectional EV charging station for buffered BESS support depicted in Section 2.2 has multimode operation. The station needs to support the bidirectional power flow during different modes of operation. There are three types of operation modes when the power is drawn from the EV battery. The converter needs to operate in standalone mode when the EV battery is supplying the house load during emergency by maintaining constant voltage and frequency. This mode is also known as grid

forming. The output frequency is a fixed frequency which means that the frequency is given by the converter and not imposed by the grid. The converter can also operate in grid-connected mode which corresponds to charging and discharging of the EV battery from/to the grid. During charging operation, the AC/DC converter adjusts its output voltage based on the input from the grid, which allows it to transfer power to the battery in a controlled manner. This mode of operation of inverter is also known as grid following mode. During discharge or V2G mode, the DC/AC converter converts the DC power from the battery into AC power as an inverter. The AC power is then fed back into the grid through the grid-connected inverter. The DC/AC inverter adjusts its

output voltage and frequency to match the grid, which ensures that the power transfer is synchronized with the grid. The control schemes for charging, V2G and V2H are explained in the subsections below. illustrates a charging station that is composed of multiple AC/DC converter modules connected in parallel.

4.1.1 Off-Grid Inverter Mode (V2H Mode)

In this mode, the off-grid inverter generates constant magnitude and frequency of three-phase voltage under grid forming mode control. This mode works when house load is not connected to the main grid, thus it supplies its own local load from the renewable energy source or energy storages.

4.1.2 EV Charging Mode (G2V Mode)

In this mode, the power converter operates as a rectifier which allows the energy transfer from 3-phase grid to EV battery. The dual-loop feed forward decoupling approach is used, which comprises the outer voltage control loop and inner current loop for the d-axis and q-axis current control. The first loop is a fast current loop, which controls the current flowing through the active front end by generating control signals (duty cycle). This loop is used to respond quickly to changes in load current and to limit current harmonics. The second loop is a slower voltage loop, which controls the voltage across the DC bus by generating the current reference (I_{dref}). This loop is used to maintain a constant DC bus voltage and to control the power factor. The feedforward part of the control strategy is used to compensate for the voltage drop across the inductance of the AC side inductors. By measuring the AC side voltage and current, the feedforward control calculates the voltage drop across the inductance and adds this value to the voltage reference of the voltage loop. This compensation improves the accuracy of the voltage control and reduces distortion.

4.1.3 EV Battery discharging mode (V2G Mode)

In this mode, the inverter varies the injected active and reactive power depending on the voltage and frequency of the main grid. If the voltage and frequency of the main grid are at their nominal values of 400V and 50 Hz, the inverter injects the rated active and reactive power values. However, if there is any variation in voltage or frequency, the control of the inverter responds by varying the injected power to maintain the stability of the main grid.

4.2 Role of controller

In a photovoltaic (PV)-based off-board electric vehicle (EV) charging system, maintaining a constant DC link voltage and ensuring stable battery charging are critical requirements. The voltage output of the PV array fluctuates continuously due to changes in solar irradiance and temperature, leading to instability in the power delivered to the converter stages and the EV battery. To overcome this challenge, intelligent control systems are employed to regulate converter duty cycles and maintain system stability. Among the most widely used controllers in power electronics are the Proportional-Integral (PI) controller and the Fuzzy Logic Controller (FLC).

Both controllers play vital roles: the PI controller provides accurate steady-state performance, while the fuzzy logic controller adds adaptability and robustness against nonlinearities. The combination of these two methods—known as a Hybrid PI-Fuzzy Controller—forms the core of the control strategy proposed for grid connected modular inverter charging station. The hybrid controller improves response time, reduces overshoots, and ensures efficient power transfer between the EV battery, BESS and Grid.

4.3 Architecture and Operations of FLC System:

The basic architecture of a fuzzy logic controller is shown in Figure 2. The principal components of an FLC system is a fuzzifier, a fuzzy rule base, a fuzzy knowledge base, an inference engine, and a defuzzifier. It also includes parameters for normalization. When the output from the defuzzifier is not a control action for a plant, then the system is a fuzzy logic decision system. The fuzzifier present converts crisp quantities into fuzzy quantities. The fuzzy knowledge base stores the knowledge about all the input-output fuzzy relationships. It includes the membership functions defining the input variables to the fuzzy rule base and the out variables to the plant under control. The inference engine is the kernel of an FLC system, and it possesses the capability to simulate human decisions by performing approximate reasoning to achieve the desired control strategy. The defuzzifier converts the fuzzy quantities into crisp quantities from an inferred fuzzy control action by the inference engine.

The inputs are crisp (non-fuzzy) numbers limited to a specific range.	All rules are evaluated in parallel using fuzzy reasoning.	The results of the rules are combined and distilled (defuzzified).	The result is a crisp (non-fuzzy) number.
---	--	--	---

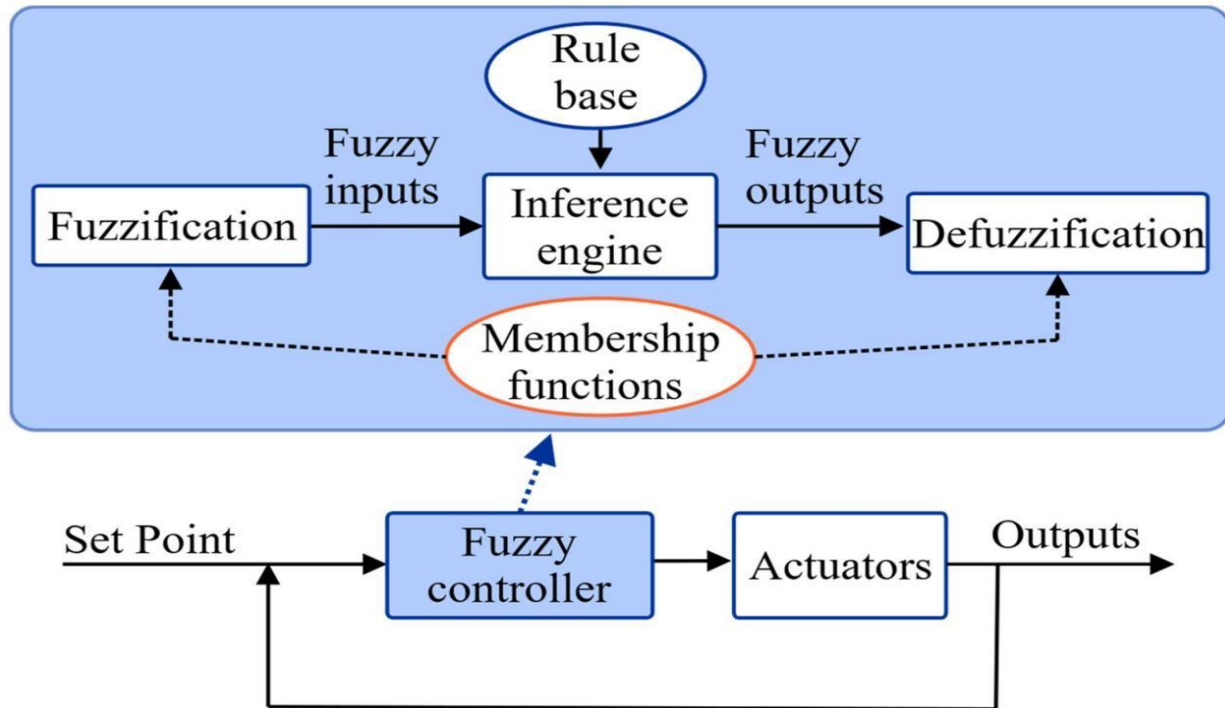


Fig 4.3 - Basic structure of a FLC

Fuzzy logic controllers (FLCs) manage bidirectional power flow in DC-AC systems by using fuzzy logic to determine the appropriate switching patterns for IGBTs to smoothly regulate power, ensuring efficient power exchange between sources and loads like electric vehicles or micro-grids. The FLC's three main steps—fuzzification of inputs, rule-based inference using a fuzzy rule base, and defuzzification of the output to crisp signals—allow it to adapt to changing conditions and minimize power disturbances without needing complex mathematical models or linearization assumptions, making it suitable for applications like EV charging and grid interface.

4.4 How FLC works:

4.4.1 Inputs: The fuzzy logic controller receives inputs such as voltage error, current error, and power flow direction.

4.4.2 Fuzzification: These inputs are converted into linguistic variables (e.g., "too high," "too low," "positive") and assigned degrees of membership to fuzzy sets. The first step involves converting the crisp

input values (Error (e) and rate of change of error (Δe)) into fuzzy linguistic variables using membership functions. The input ranges are divided into fuzzy sets such as Negative Big (NB), Negative Medium (NM), Negative Small (NS), Zero (ZE), Positive Small (PS), Positive Medium (PM), and Positive Big (PB). These sets are represented by triangular membership functions.

4.4.3 Fuzzy Rules: A set of "IF-THEN" rules, based on expert knowledge and system behavior, are applied. For example, a rule might state: "IF the DC link voltage is too high AND the power is flowing to the grid, THEN reduce the PWM duty cycle".

For example:

4.4.3.1 If (e is Positive Big) and (Δe is Positive Small), then (Δu is Positive Big).

4.4.3.2 If (e is Zero) and (Δe is Zero), then (Δu is Zero).

These rules define how the system should react under different conditions and form the core of fuzzy reasoning.

4.4.4 Inference Engine: The controller uses these rules to determine the degree to which each rule applies to the current input conditions. The inference engine processes the input fuzzy variables through the rule base to generate corresponding output fuzzy sets. The most common inference mechanism is Mamdani-type fuzzy inference, which uses the min-max composition method.

4.4.5 Defuzzification: The fuzzy outputs from all applicable rules are combined and converted into a precise, crisp output signal. Finally, the fuzzy output sets are converted back into a crisp value (Δu) using techniques such as the centroid method. This output determines how the duty ratio of the converter should be adjusted to achieve the desired voltage regulation.

4.4.6 IGBT Switching: This crisp output is then used to generate the appropriate control signals (e.g., pulse width modulation - PWM) that precisely switch the Insulated Gate Bipolar Transistors (IGBTs) in the bidirectional converter, thereby controlling the direction and magnitude of power flow.

4.5 Advantages of FLC: FLCs provide smooth transitions between operating modes, minimizing disturbances in power flow and voltage regulation. They are well-suited for complex systems with variable renewable energy sources, like solar, and can handle sudden changes in load or generation without complex mathematical modeling. By adapting to system dynamics, FLCs can offer better voltage regulation, reduced output voltage distortion, and efficient power management compared to traditional controllers like PI controllers. They simplify the control design process by using linguistic rules instead of relying solely on complex mathematical equations or linearization, making them practical for various power electronics applications.

4.6 Simulink implementation of controller:

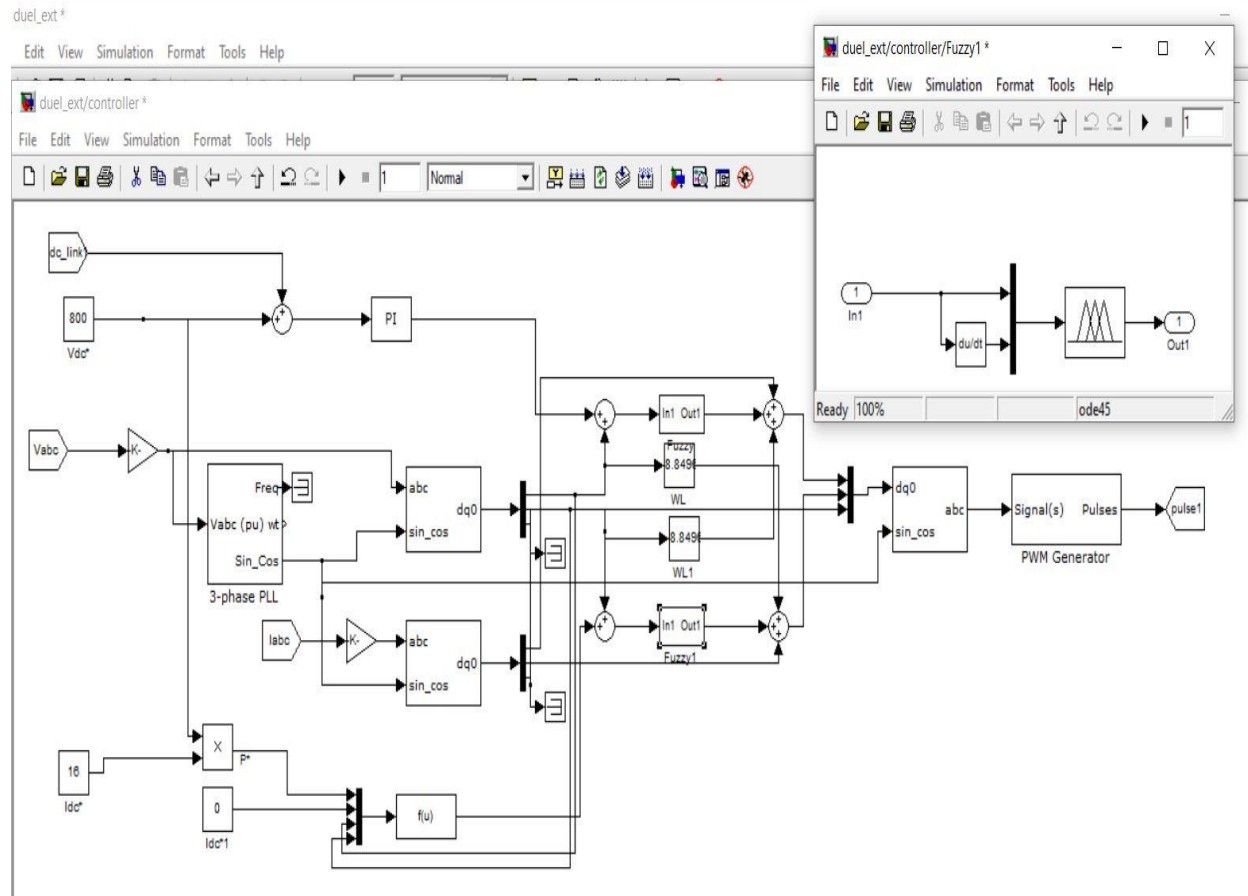


Fig 4.6.1 - Controller Simulink model

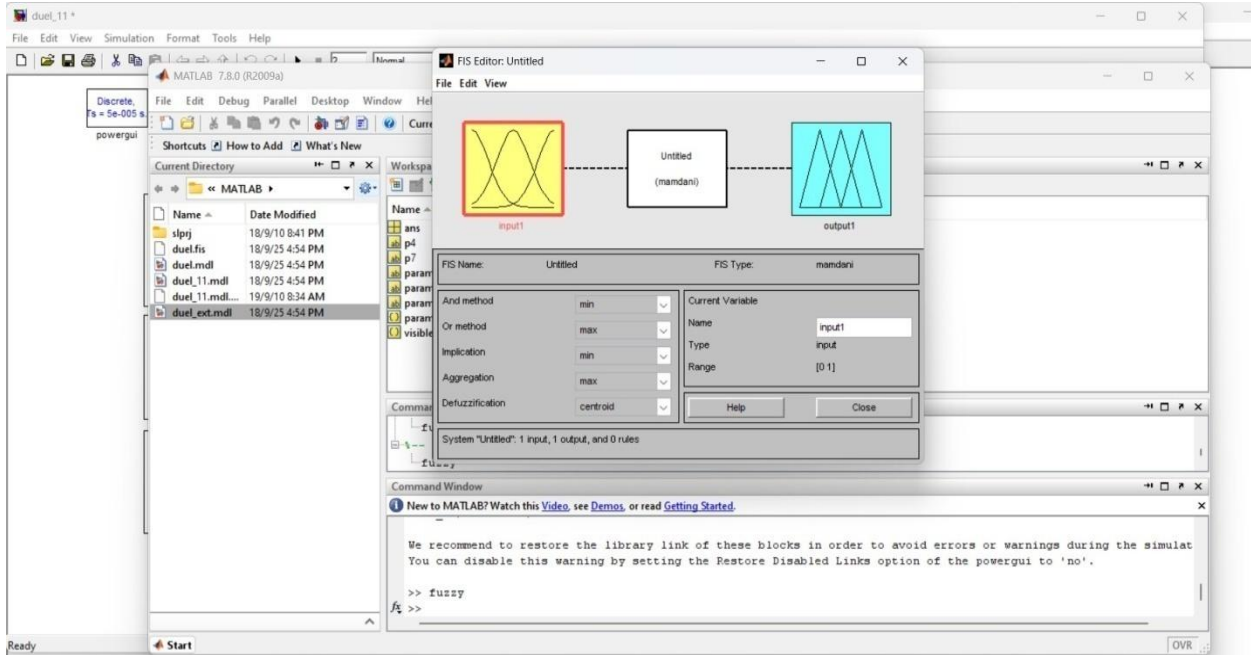


Fig 4.6.2 - Membership functions fuzzy system of save current to workspace

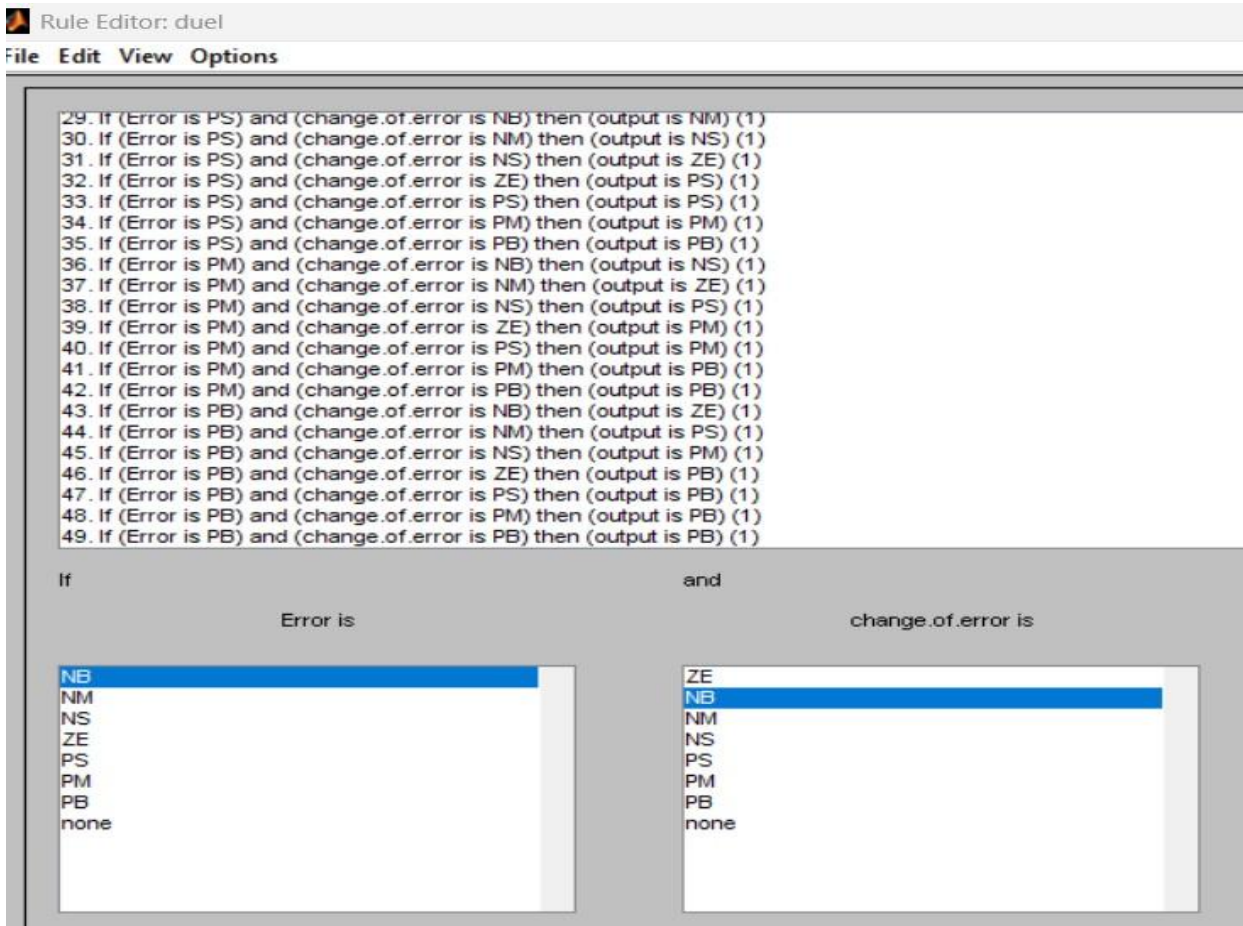


Fig 4.6.3 - Fuzzy Rule set

4.7 Fuzzy Logic Membership functions

Table 4.7 - Fuzzy Logic Truth Table

Membership Function	Δe								
		NB	NM	NS	ZE	PS	PM	PB	
MF1	NB	NB	NB	NB	NB	NM	NS	ZE	
MF2	NM	NB	NB	NB	NM	NS	ZE	PS	
MF3	NS	NB	NM	NS	NS	ZE	PS	PM	
MF4	ZE	NB	NM	NS	ZE	PS	PM	PB	
MF5	PS	NM	NS	ZE	PS	PS	PM	PB	
MF6	PM	NS	ZE	PS	PM	PM	PB	PB	
MF7	PB	ZE	PS	PM	PB	PB	PB	PB	

e – error, Δe – rate of change of error, NB – Negative Big, NM – Negative Medium, NS – Negative Small, ZE – Zero, PS – Positive Small, PM – Positive Medium, PB – Positive Big.

4.8 Electrical Vehicle and Battery Simulation block

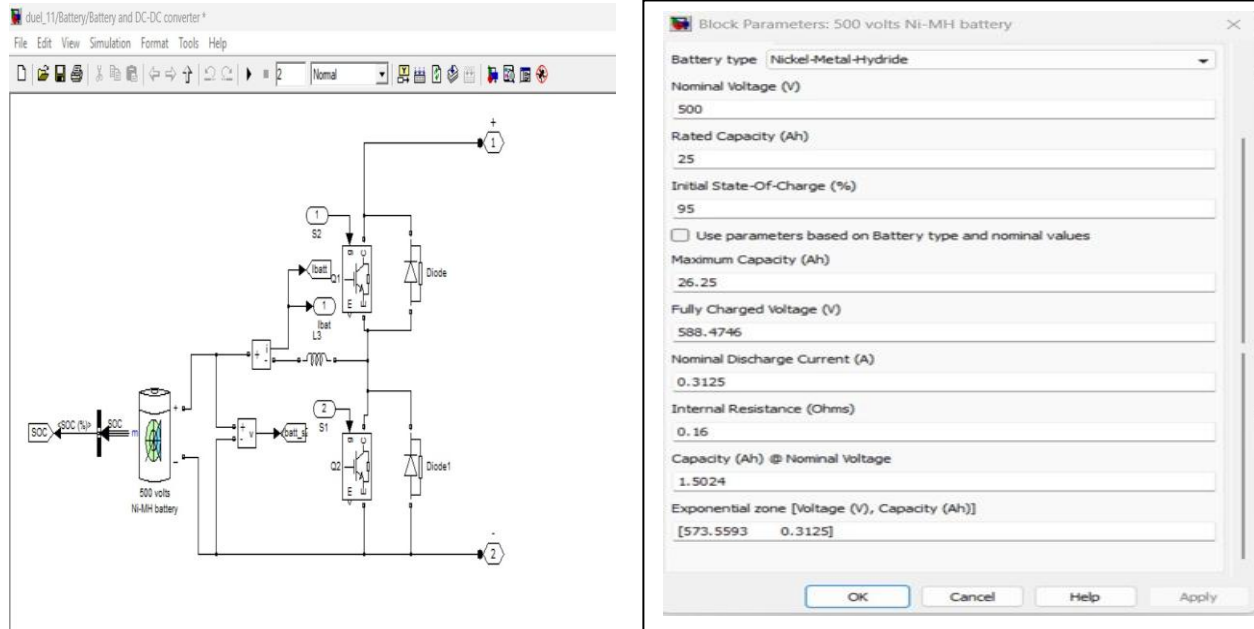


Fig 4.8 - EV Simulink mode

4.9 Proposed Simulink Model:

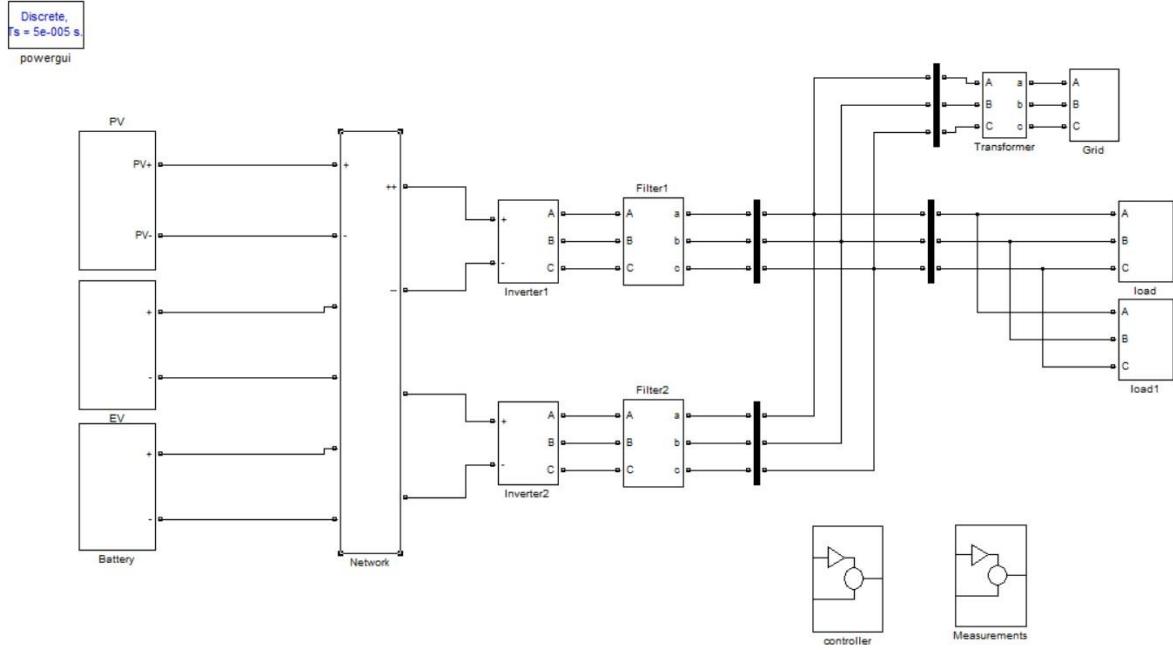


Fig 4.9.1 - Proposed Grid-Connected Inverter Integrated DC Charging Station

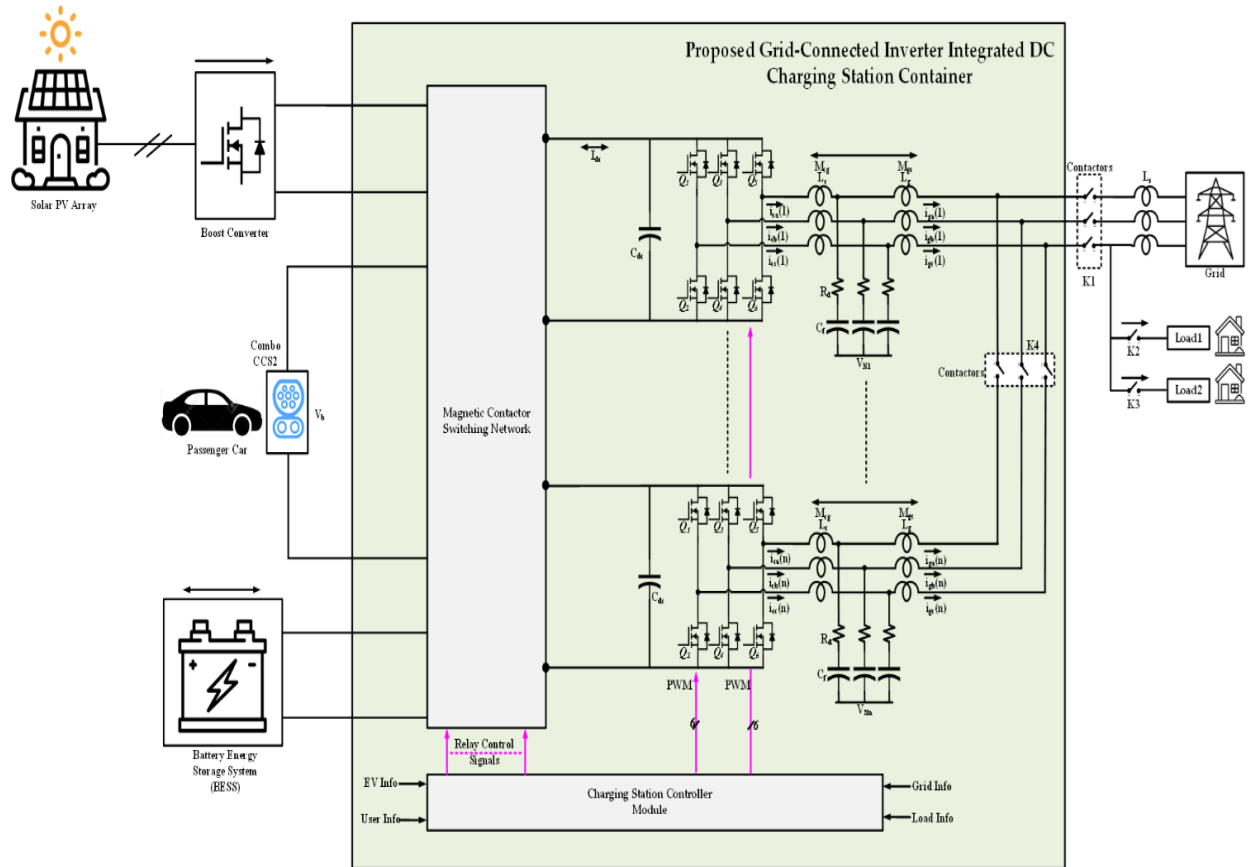


Fig 4.9.2 - Modular bidirectional DC/AC converter with LCL filter along with controller connected to grid and house load through isolator switch

4.10 Converter Module Specifications and System Parameters

Table 4.10 - Converter Module Specifications and System Parameters

Symbols	Description	Ratings
P	Converter Rated Power	20 kW
V_s	Supply voltage from grid	400 Vrms
V_{dc}	DC Link Voltage(Max)	1000 V
f_s	Switching frequency	20 kHz
L_g	Filter inductance (grid side)	1.35 mH
C_f	Filter capacitance	50 uF
L_c	Filter inductance (converter side)	0.961 mH
C_{dc}	DC-link capacitance	1000 uF
R_d	Damping resistance	0.01 Ω
-	EV Battery	100 kWh, 500 V
-	BESS	100 Kwh
-	Solar PV	10 kWp
-	Maximum Home load	38 kWh
-	3- ϕ Converter (on AC supply side)	20 KW, 400 V(L-L) at 50 Hz grid frequency

4.11 Operating mode control strategy:

The overall control algorithm of the EV and charging station is shown in Figure 4.11.1. The algorithm initiates by extracting the EV information such as EV battery SoC, battery voltage, V_b , arrival time, T_a , and departure time, T_d . If the current SoC of the EVB is less than SoC_{min} , which is a predefined value of charge needed for emergency, the EV will enter the grid-to-vehicle (G2V) mode. In this mode, the EVB

is charged with the constant current (CC) and constant voltage (CV). The charging session continues until SoC is equal to SoC_{max} which is the maximum value of charge (around 80% of SoC). The V2G mode activates based on two conditions specifically the SoC should be equal or larger than SoC_{max} and V2G consent from the EV owner. Similarly, V2H mode activation also needs V2H consent from the EV user.

4.11.1 Control Algorithm:

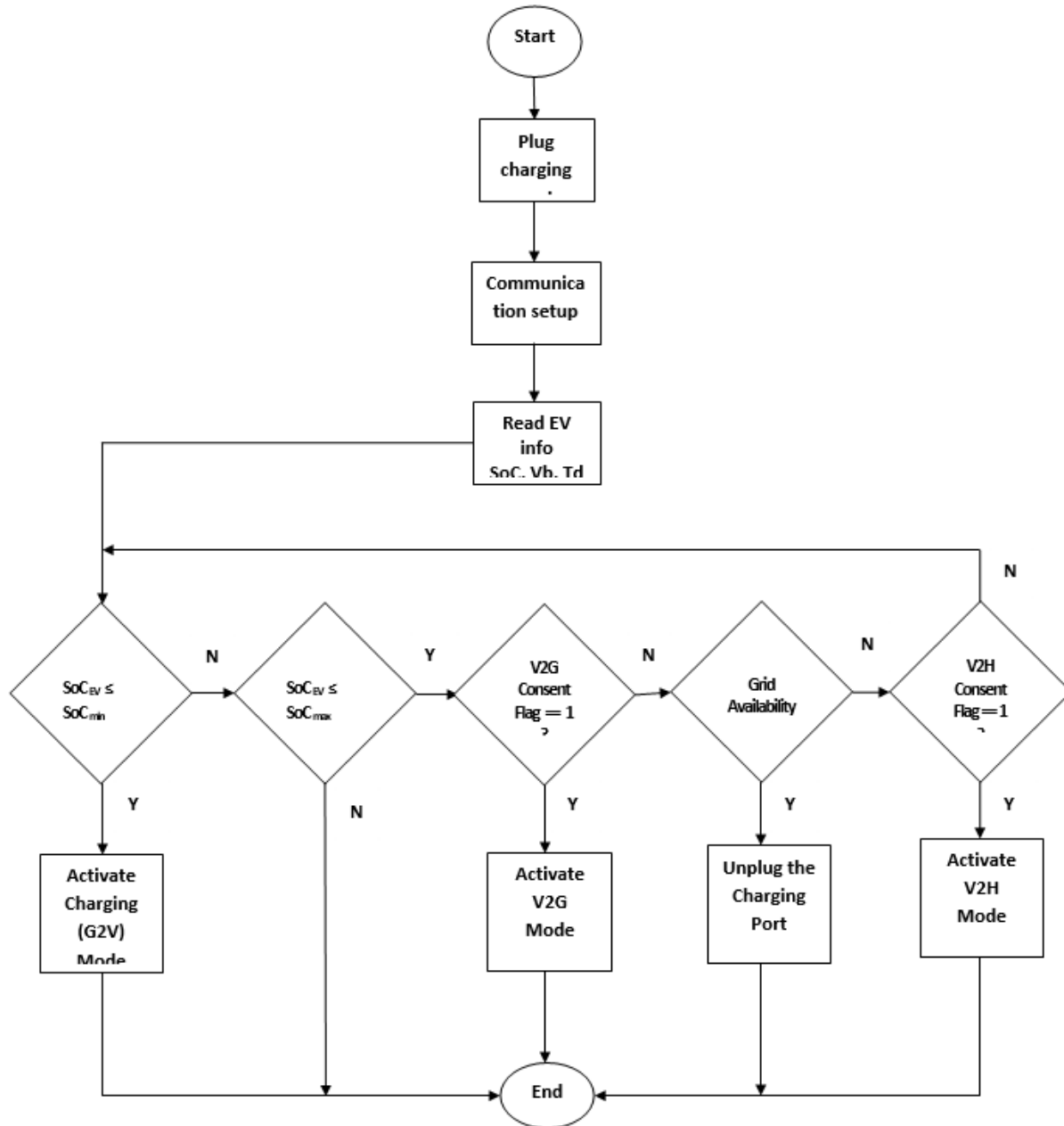


Fig 4.11.1 - Overall control algorithm to activate the operating mode of proposed system

V. RESULTS AND DISCUSSION

5.1 Overview: This section presents simulation results of the proposed bidirectional EV charging converter under the different working conditions described in the previous section. The individual converter rated power is 20 kW with 400V line-to-line voltage at 50 Hz grid frequency. The load demand is modeled around 26kW and 23kVAR until

t=0.15 sec. Then the load is increased up to 38kW and 36kVAR until t=0.25 sec.

5.2 DC and AC side performance for V2H mode including RL load transition at t=0.15 sec
 During V2H mode, the charging station operates as stand-alone off-grid inverter to supply the load. The inverter converts the DC power either from the solar PV array or the EV battery storage. The active and

reactive power response for both converters with the load demand is shown in Fig 5.2.1 The EV battery discharged to fulfill the load demand during V2H mode. The battery performance profile is depicted in Fig 5.2.2. The battery SoC should be high enough to

deliver the current demand required by the residential load. The battery SoC decreases during V2G, and the decreasing rate is high after load demand increases at $t=0.15$ sec.

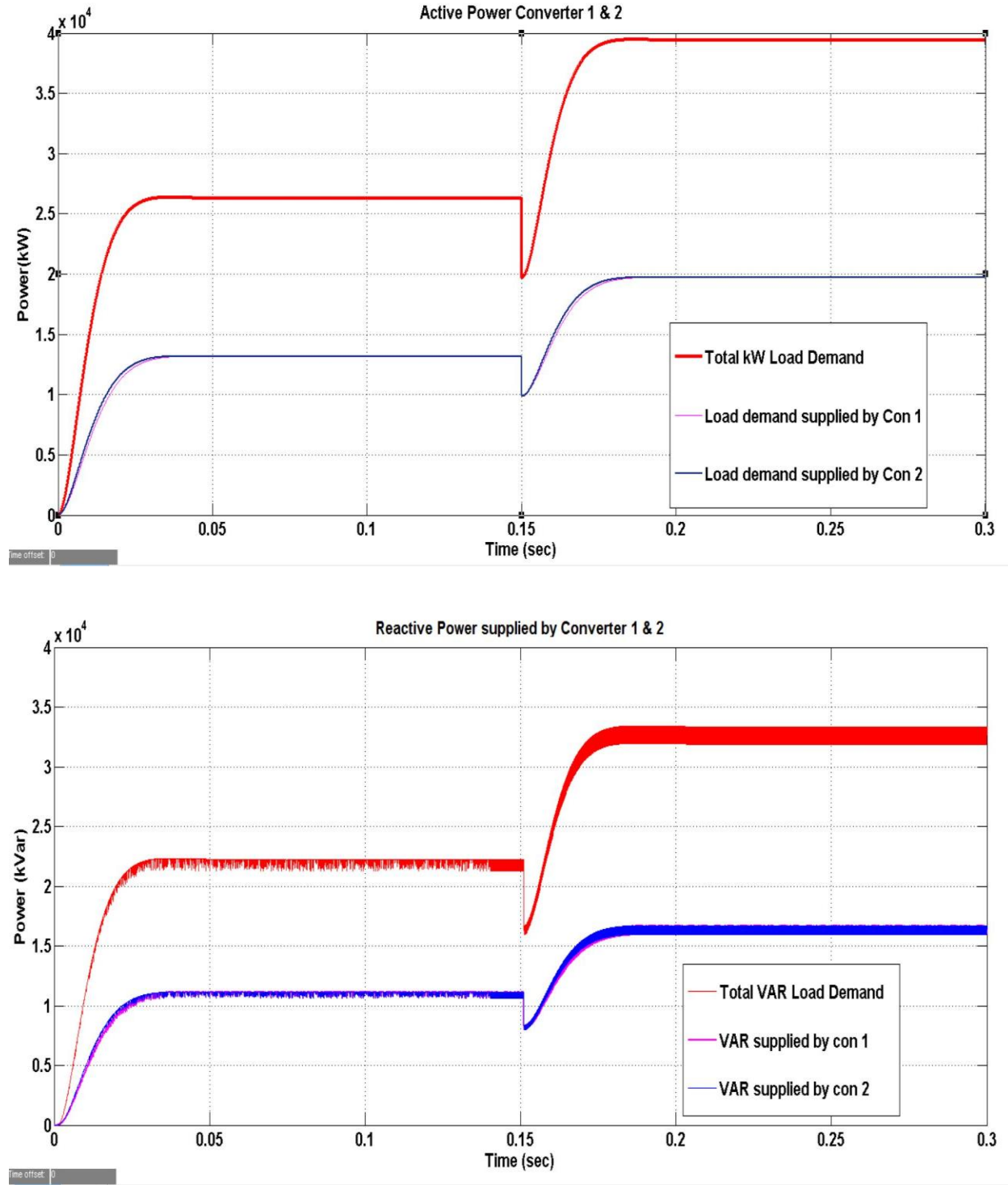


Fig 5.2.1 – Active and Reactive power profile performance during V2H mode

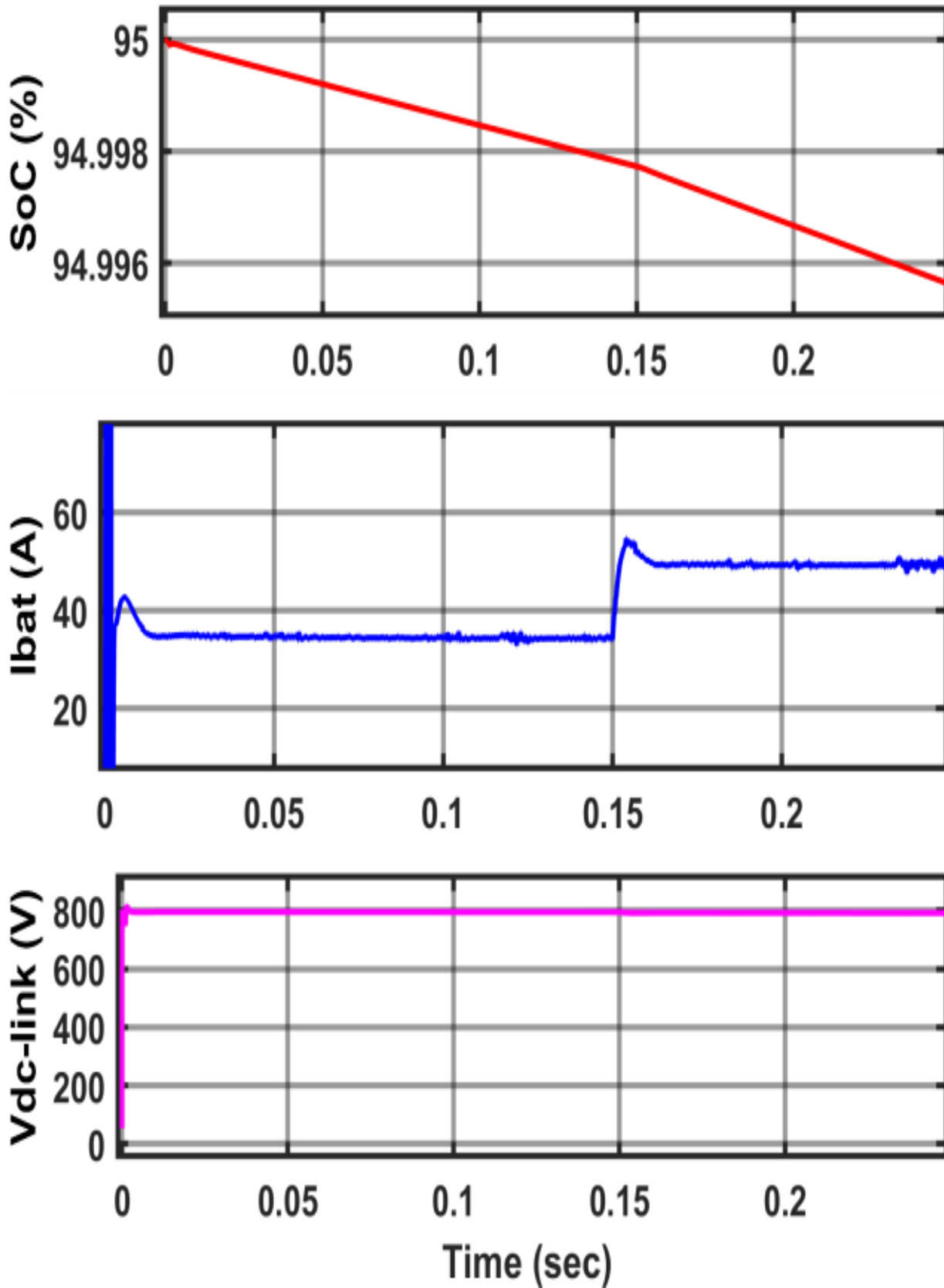


Fig 5.2.2 - EV Battery performance (Voltage, Current, and SoC) during V2H service

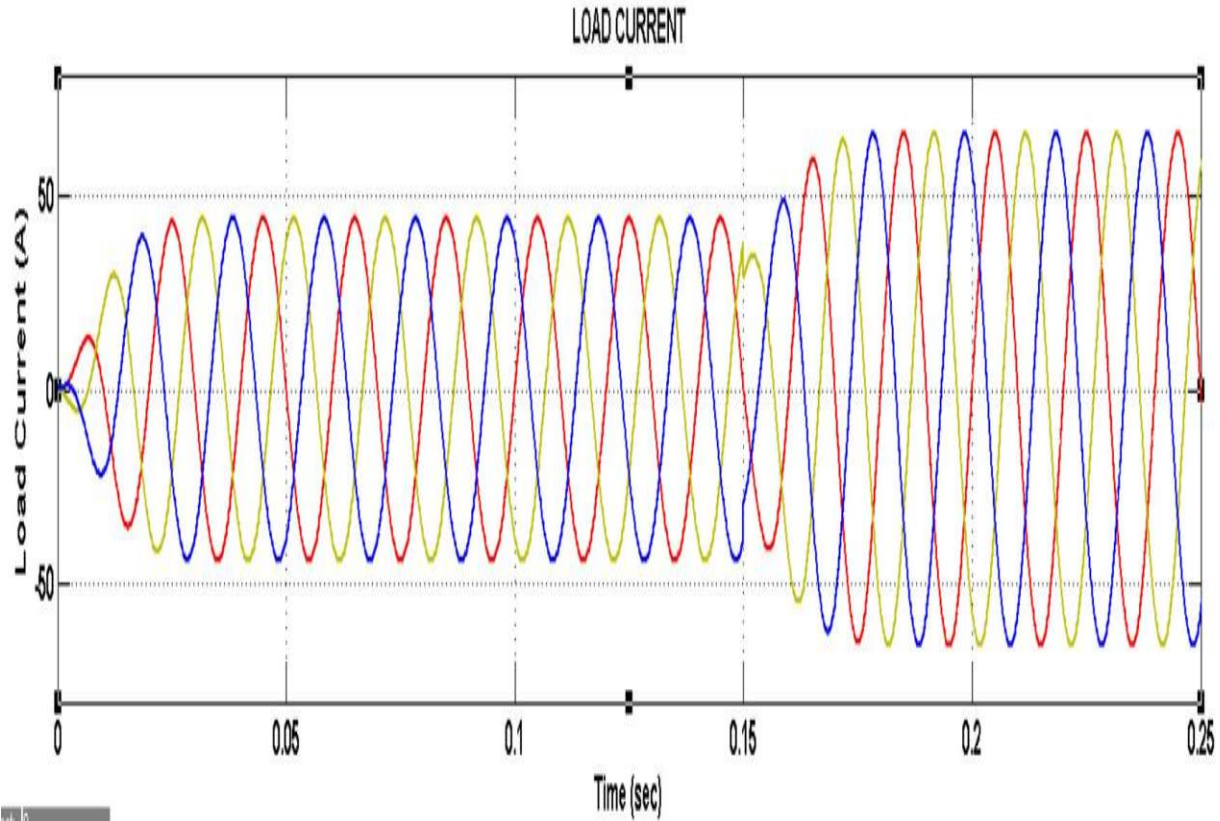


Fig 5.2.3 – Load current during V2H mode

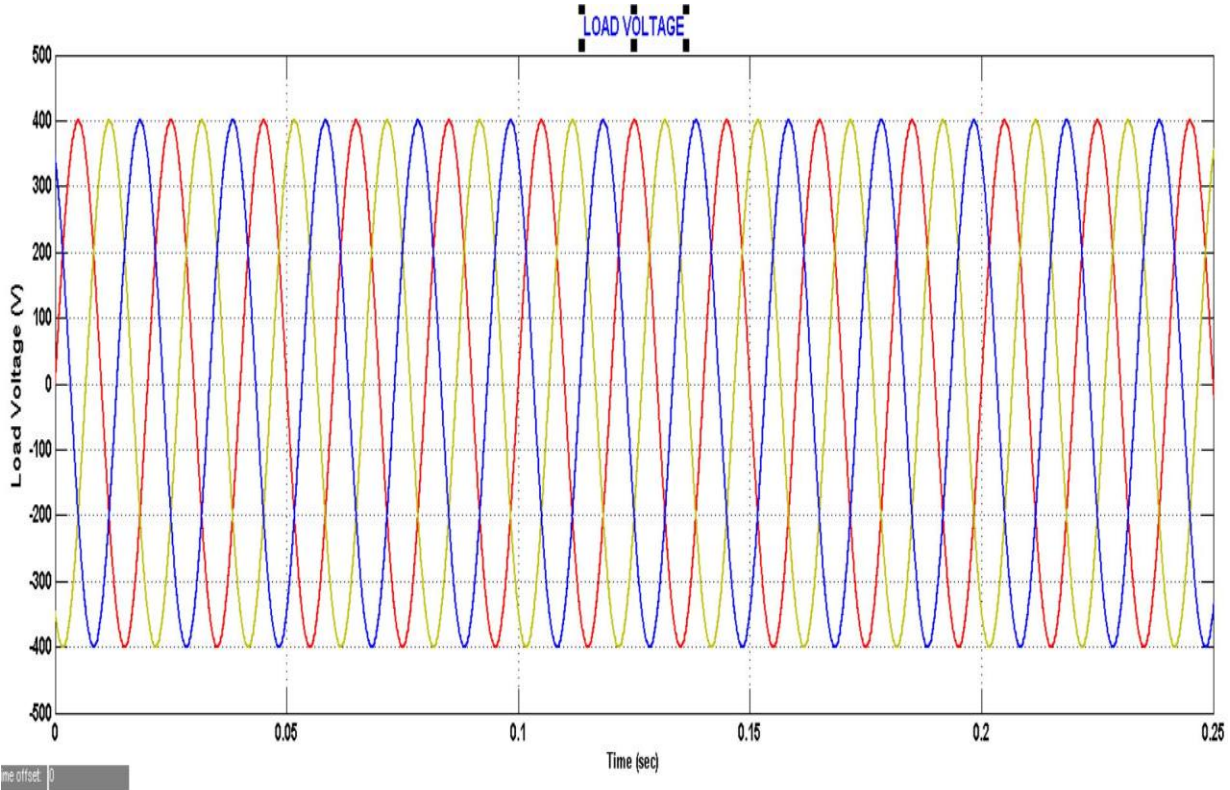


Figure 5.2.4 AC Grid voltage during V2H mode

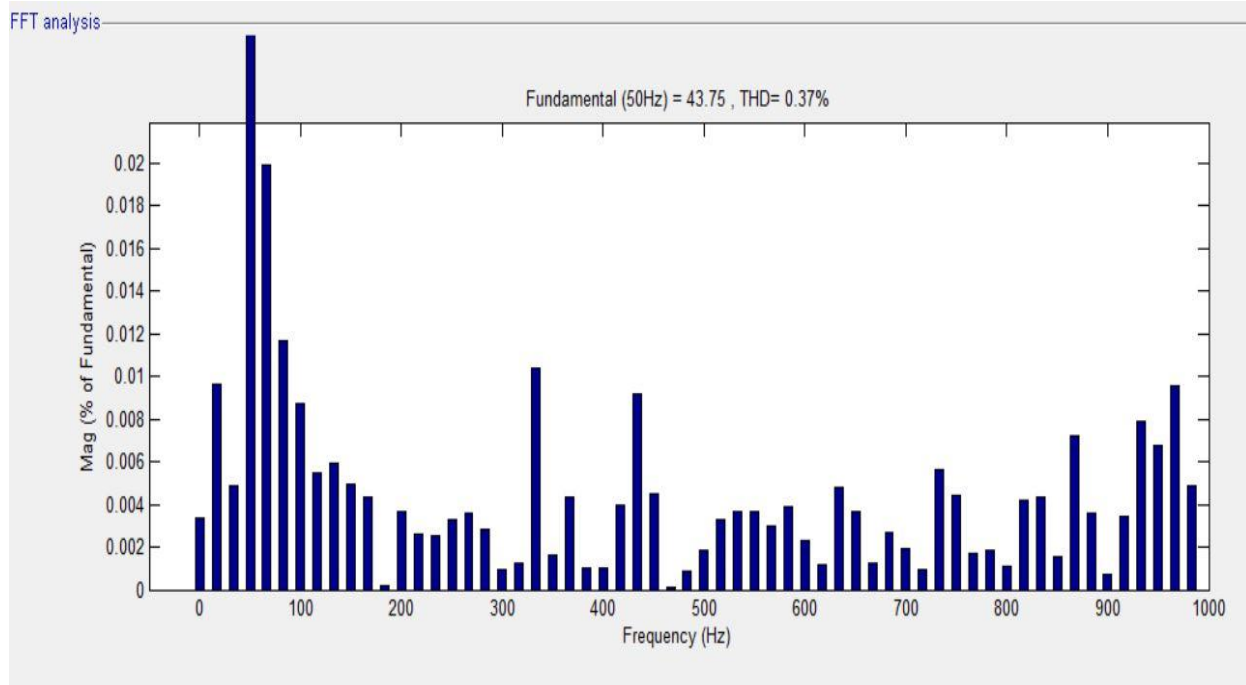
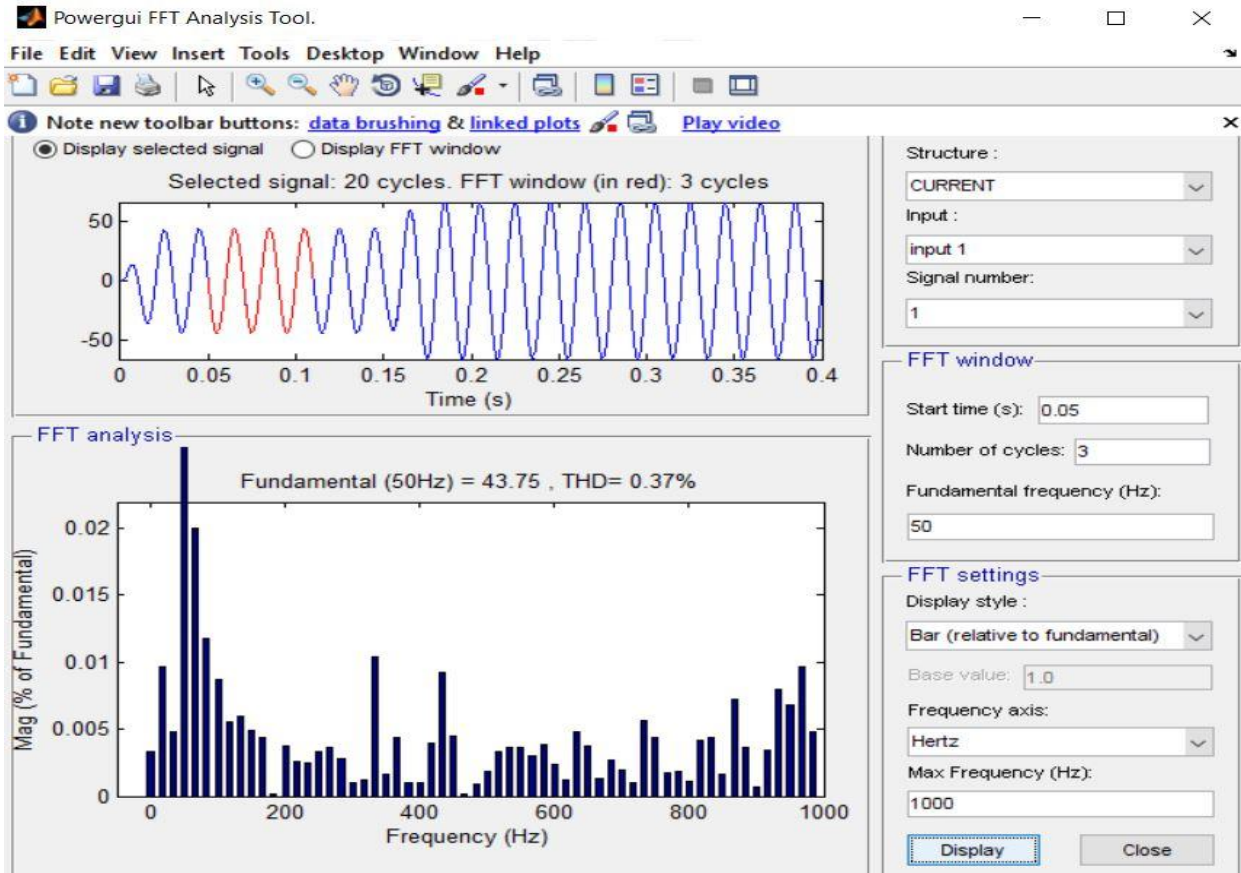


Fig 5.2.5 THD profile in load current during V2H service

5.3 The Battery performance during charging mode which change into Vehicle-to-Grid (V2G) mode at $t=0.15$ sec.

Charging station is also capable of operating in charging and V2G mode to charge the battery during off-peak period and sends back the battery power to the grid during the higher energy price. The battery performance during charging and V2G mode is illustrated in Figure 21. The EV battery is considered

with nominal voltage is 340V and 100 Ah rated capacity. The battery is charged using the grid with 15A (0.3C) charging current until $t=0.15$ sec. The charging rate is around 5.5kW which means the battery will be fully charged in 3 hours. After $t=0.15$, the EV battery is discharged to the grid at the same rate (5.5kW). The battery voltage decreases from 370V to 364V during V2G.

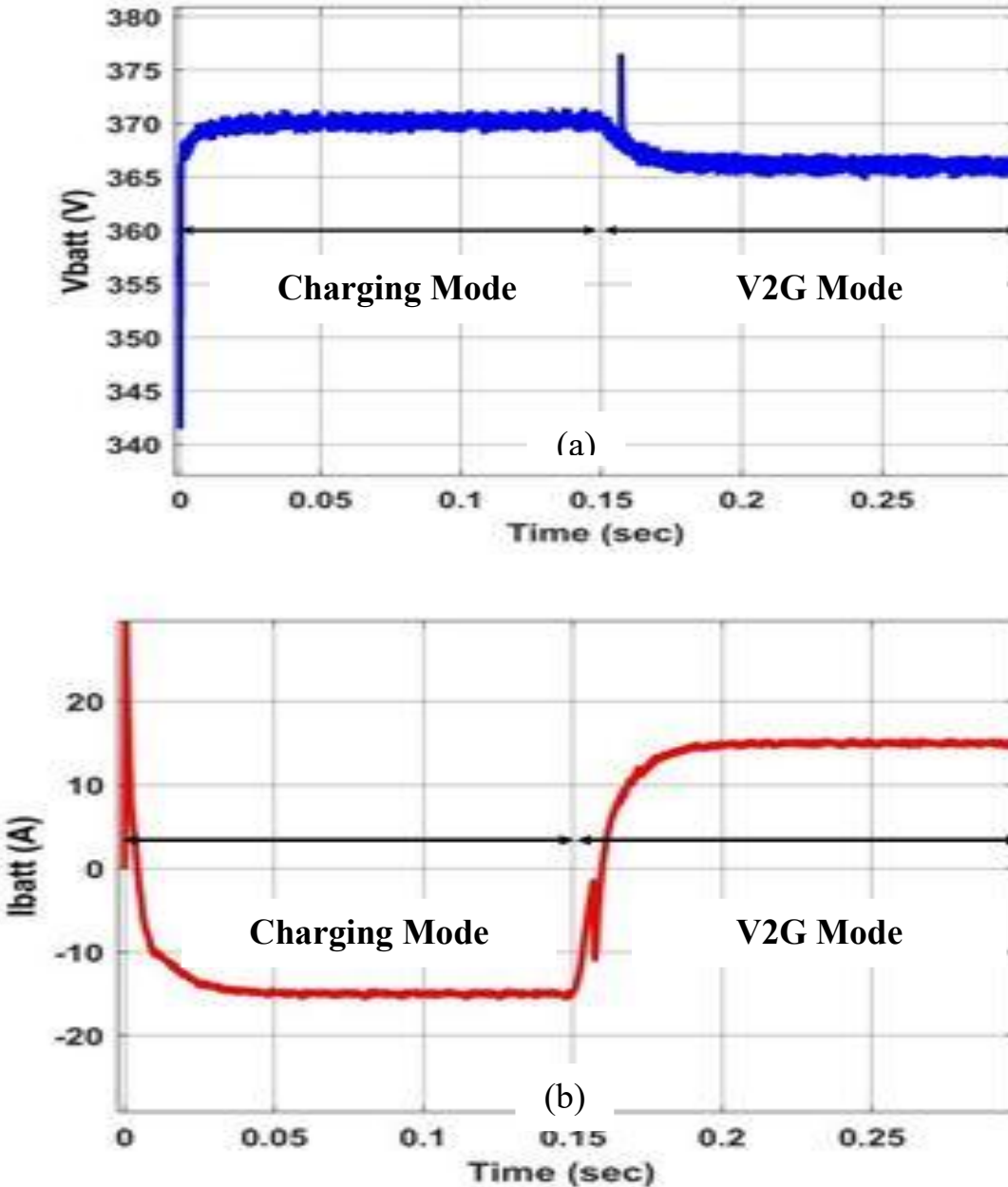


Fig 5.3.1 EV Battery (a) Voltage and (b) Current

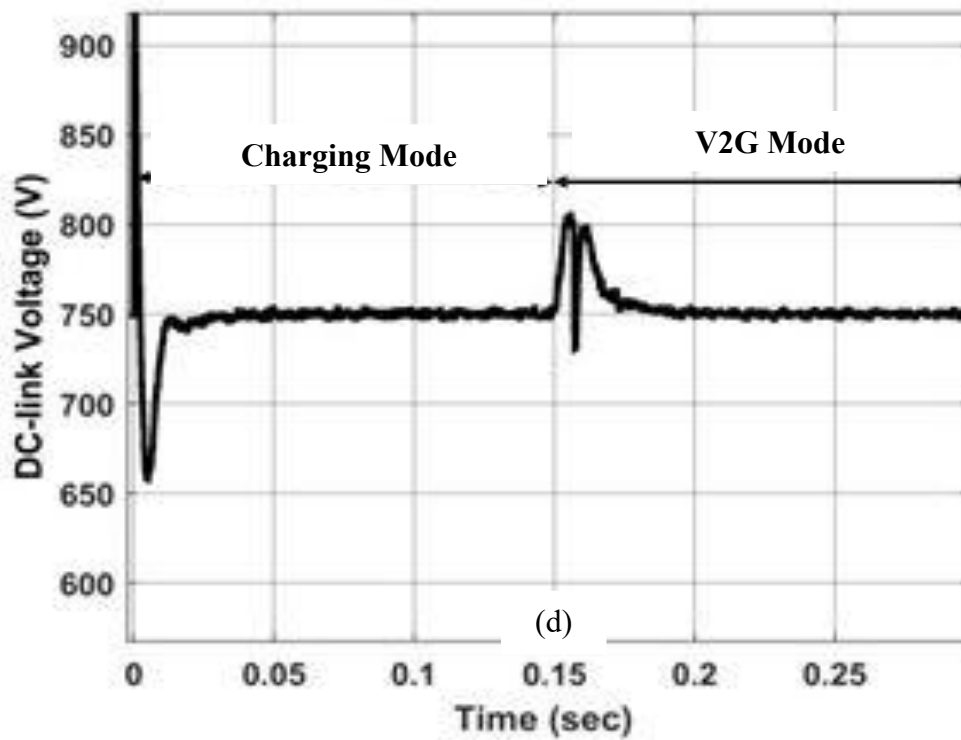
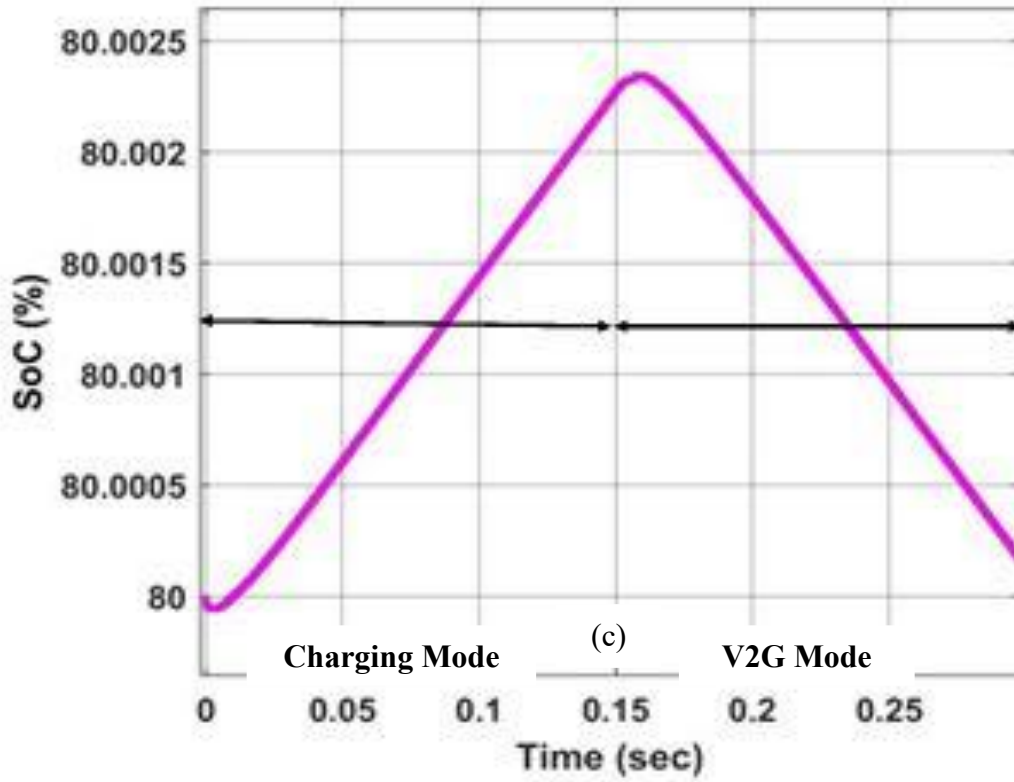


Fig 5.3.1 - (c) State of Charge (SoC) profile of battery and (d) DC-Link voltage

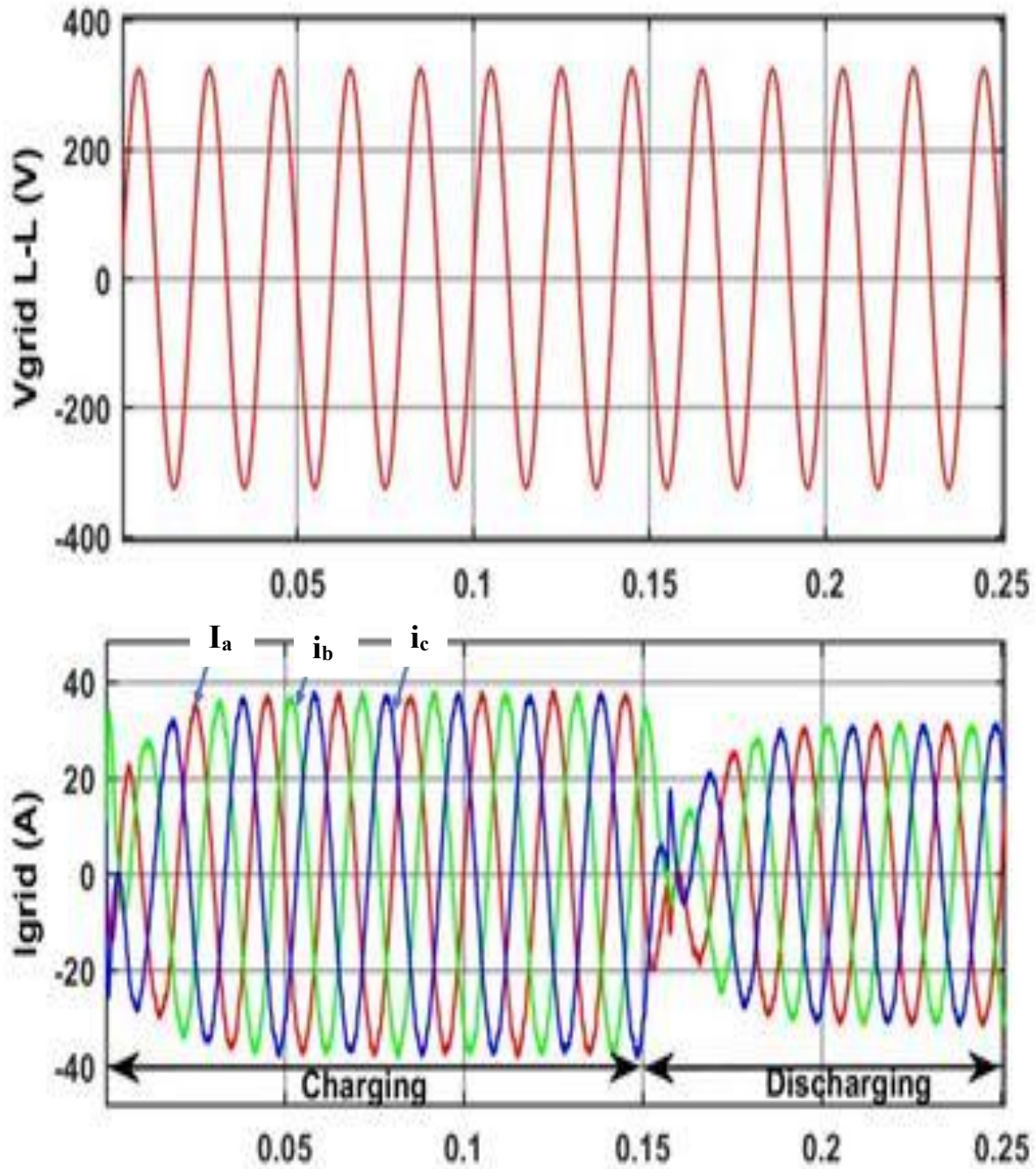


Fig 5.3.3 - AC voltage and Current profile during to charge and discharge the EV battery during charging and V2G mode

The charging current is 15A and charging rate is around 5.55 kW. Moreover, the battery voltage decreases during the battery power sends back to the grid at a 5 kW rate. The battery power profile is shown in Fig 5.3.4.

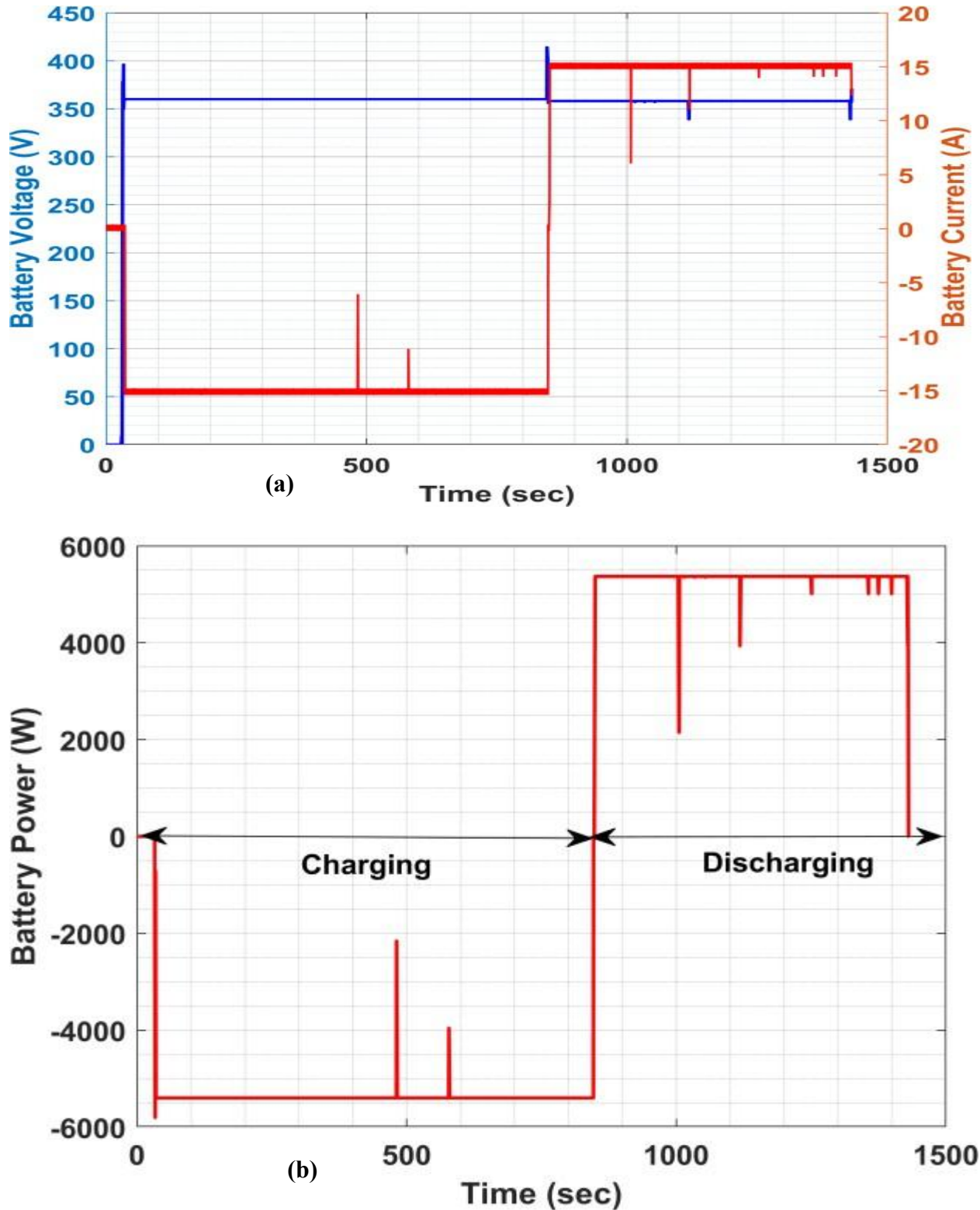


Fig 5.3.4 - Battery emulator performance during charging and V2G mode

(a) Battery voltage and current (b) battery power profile for charging and V2G mode

Table 5.3 Efficiency calculations for G2V and V2G mode of operation

Parameter	G2V mode of operation
Initial SoC	35 %
I_b	15 A
V_b	370
Power	5.5 KW
EV charging rate	5.55 KW
Input Power from AC Grid	6.6 KW
Efficiency	$5.5/6.3 = 87\%$

Parameter	V2G mode of operation
Initial SoC	80.02 %
I_b	15 A
V_b	400
EV discharging rate	8.77 KW
Output AC power	8.3 KW
Efficiency	$8.3/8.77 = 94.64\%$

VI. CONCLUSION AND FUTURE WORK

6.1 Conclusion: This research work has presented the design, modeling, and performance analysis of an Integrated Bidirectional Charging Station (IBCS) suitable for residential and small-scale community smart grid applications. The proposed system was conceptualized, simulated, and validated to demonstrate its ability to serve as an efficient and intelligent energy conversion interface between electric vehicles (EVs), renewable energy sources (RES) such as solar photovoltaic (PV) systems, and the utility grid. The system employs a grid-connected modular inverter architecture with bidirectional power flow capability, enabling Vehicle-to-Grid (V2G), Vehicle-to-Home (V2H), and Grid-to-Vehicle (G2V) operations. Through the integration of advanced hybrid control techniques based on Proportional-Integral (PI) and Fuzzy Logic Control (FLC), the system achieves enhanced dynamic performance, superior voltage regulation, and high-power quality, meeting the requirements of emerging smart grid environments.

The increasing adoption of electric vehicles and renewable distributed energy systems has created new challenges in grid stability, energy utilization

efficiency, and load management. To address these challenges, the present study developed a multi-functional inverter-based bidirectional converter that can manage the flow of power between multiple sources and sinks.

6.1.1 The IBCS designed in this research serves three main purposes:

6.1.1.1 Electric Vehicle Charging Interface – providing controlled and efficient charging from either grid or renewable energy sources.

6.1.1.2 Grid Support and Peak Load Management – allowing discharge of stored energy from EV batteries to support the grid during high demand periods.

6.1.1.3 Renewable Energy Integration – enabling direct utilization of PV-generated power for both EV charging and household supply.

A modular inverter topology was adopted to achieve flexibility, scalability, and efficient energy sharing across these interfaces. The inverter functions as a grid-interfacing converter, managing the energy exchange between the dc-link, battery, PV array, and AC grid. The modular design also facilitates easy extension of the system for higher capacities and multi-vehicle charging applications.

6.1.2 Control Strategy and Dynamic Performance

The control architecture forms the core of the system’s performance. In this study, a hybrid PI-Fuzzy Logic Controller (FLC) was implemented for regulating the dc-link voltage and managing transient behavior during bidirectional power transitions. The conventional PI controller, though effective for steady-state regulation, exhibits limitations under nonlinear or rapidly changing conditions such as fluctuating loads, renewable intermittency, and grid disturbances. To overcome these limitations, the PI controller was complemented with an FLC, which introduces adaptive and intelligent control characteristics without requiring an exact mathematical model of the system.

The fuzzy logic component dynamically adjusts control actions based on variations in voltage error and its rate of change, improving transient response and minimizing overshoot. Simulation results reveal that the hybrid controller maintains the dc-link voltage closely around **750 V**, with minimal ripple and fast recovery after disturbances. Compared with the conventional PI-only controller, the hybrid approach exhibits improved dynamic stability,

enhanced damping of oscillations, **and** faster settling time, ensuring smooth transitions between charging and discharging modes.

6.1.3 Quantitative Results and Analysis

Comprehensive simulations were carried out using MATLAB/Simulink to evaluate the system under different operating modes — Vehicle-to-Home (V2H), Vehicle-to-Grid (V2G), and Grid-to-Vehicle (G2V). The analysis considered both steady-state and dynamic conditions, with performance metrics focusing on voltage regulation, efficiency, and Total Harmonic Distortion (THD).

6.1.3.1 In V2H mode, the inverter supplied power to a resistive load with a measured THD of approximately 0.37%, demonstrating excellent power quality and minimal harmonic content in compliance with IEEE 519 standards.

6.1.3.2 In V2G mode, the system achieved a THD of 0.43%, confirming stable and clean power injection into the grid during discharge operation. The EV battery discharged at a rate of 5.5 kW, causing a slight voltage decrease from 370 V to 364 V, with an initial State-of-Charge (SoC) of 80.002%.

6.1.3.3 The dc-link voltage remained stable at approximately **750 V** with the hybrid FLC ensuring accurate regulation and minimal ripple compared to the PI-only configuration.

6.1.3.4 During charging (G2V) mode, when power was drawn from the grid, the system achieved a charging efficiency of around 87%, drawing 6.3 kW from the AC grid.

6.1.3.5 During V2G operation with SoC of 88.02%, the inverter delivered 8.3 kW to the AC side while consuming 8.77 kW from the EV battery, yielding a V2G efficiency of 94.64%.

These results confirm that the proposed hybrid control not only stabilizes the system under different operational modes but also enhances the overall efficiency, transient behavior, and harmonic performance of the bidirectional charging system.

6.1.4 System Performance

The simulation outcomes validate the robustness of the proposed inverter and control strategy. The system consistently demonstrates low harmonic distortion, stable dc-link voltage, and smooth power flow transitions, even under dynamically changing load and grid conditions. The fuzzy logic controller plays a pivotal role in improving transient performance by automatically adapting to varying

system parameters. Its rule-based inference mechanism provides faster correction capability, minimizing error accumulation and ensuring optimal steady-state performance.

The dynamic adaptability of the controller also contributes to improved resilience under grid disturbances, enabling the system to maintain synchronization and voltage stability during fault conditions or supply interruptions. This capability is particularly valuable in smart grid environments where bidirectional energy flows and variable renewable generation can introduce complex dynamic behaviors.

Furthermore, the scalability of the modular inverter topology ensures that the proposed system can be extended for community-level applications. Multiple IBCS units can be interconnected to form a local microgrid, where each station contributes to voltage support, reactive power compensation, and peak load reduction. Such integration promotes the decentralization of energy management and supports grid stability during high-demand periods.

6.1.5 Significance for Smart Residential Energy Systems

The integration of electric vehicle charging infrastructure with distributed renewable energy sources represents a major step toward realizing the vision of intelligent and sustainable smart grids. The proposed IBCS system addresses several key challenges:

6.1.5.1 **Peak Load Reduction:** By enabling controlled V2G operation, stored energy in EV batteries can be released during peak demand, reducing strain on the grid and flattening the demand curve.

6.1.5.2 **Renewable Energy Utilization:** The inverter facilitates maximum utilization of locally generated PV power, reducing dependence on centralized generation and improving energy self-sufficiency.

6.1.5.2 **Power Quality Improvement:** The achieved THD values below 0.5% highlight excellent harmonic performance, ensuring compatibility with sensitive home electronics and compliance with power quality standards.

6.1.5.3 **Energy Efficiency and Sustainability:** The measured efficiencies of 87% (charging) and 94.64% (discharging) confirm the potential for significant energy savings and improved system reliability.

Overall, the research underscores the feasibility of employing EVs as dynamic energy assets rather than passive loads, thus redefining the role of EVs in future energy ecosystems.

The comprehensive simulation analysis verifies that the system achieves excellent power quality (THD < 0.5%), high conversion efficiency (up to 94.64%), and robust dc-link voltage regulation (≈ 750 V) under varying conditions. These results affirm that the proposed inverter configuration and control methodology provide a practical pathway toward sustainable, resilient, and intelligent residential energy ecosystems.

Ultimately, this work contributes to advancing the integration of electric mobility, renewable energy, and smart grid technologies — supporting the global transition toward a low-carbon, energy-efficient future.

6.2 Future work

This section describes that potential limitations of the suggested DC charging solution when integrated with a grid connected inverter. To address these limitations, we propose the incorporation of a battery management system utilizing optimization and control algorithms. Such an approach aims to prolong the battery's service life. Additionally, software and hardware can be developed to monitor the health status of the battery and estimate its remaining service life. By implementing this system, EV owners can receive timely notifications before the battery reaches the end of its life, enabling them to take appropriate actions to ensure energy continuity.

REFERENCES

- [1] S. Kim and F.-S. Kang, "Multifunctional onboard battery charger for plug-in electric vehicles," *IEEE Trans. Ind. Electron.*, vol. 62, no. 6, pp. 3460–3472, Jun. 2015, doi: 10.1109/TIE.2014.2376878.
- [2] N. Naik and C. Vyjayanthi, "Optimization of vehicle-to-grid (V2G) services for development of smart electric grid: A review," in *Proc. Int. Conf. Smart Gener. Comput., Commun. Netw.*, Pune, India, Oct. 2021, pp. 1–6, doi: 10.1109/SMARTGENCON 51891.2021.9645903.
- [3] R. V. S. E. Shravan and C. Vyjayanthi, "Active power filtering using interlinking converter in droop controlled islanded hybrid AC–DC microgrid," *Int. Trans. Electr. Energy Syst.*, vol. [4] S. Shao, L. Chen, Z. Shan, F. Gao, H. Chen, D. Sha, and T. Dragicevic, "Modeling and advanced control of dual-active-bridge DC–DC converters: A review," *IEEE Trans. Power Electron.*, vol. 37, no. 2, pp. 1524–1547, Feb. 2022, doi: 10.1109/TPEL.2021.3108157.
- [5] M. Gopahanal Manjunath, V. Chintamani, and C. Modi, "A real-time hybrid battery state of charge and state of health estimation technique in renewable energy integrated microgrid applications," *Int. J. Emerg. Electr. Power Syst.*, vol. 18, pp. 1–10, May 2022, doi: 10.1515/ijeeps-2021-0434.
- [6] L. Zheng, X. Han, Z. An, R. P. Kandula, K. Kandasamy, M. Saeedifard, and D. Divan, "SiC-based 5-kV universal modular soft-switching solid-state transformer (M-S4T) for medium-voltage DC microgrids and distribution grids," *IEEE Trans. Power Electron.*, vol. 36, no. 10, pp. 11326–11343, Oct. 2021, doi: 10.1109/TPEL.2021.3066908.
- [7] Development and validation of an integrated EV charging station with grid interfacing inverter [accessed on 23 Oct, 2023].
- [8] De Lijn to buy up to 1,250 electric buses within 6 years" Available on <https://www.electrive.com/2022/03/31/de-lijn-to-procure-up-to1250-electric-buses-within-six-years/> [accessed on 28 Feb, 2023].
- [9] Liberos, M.; González edina, R.; Patrao, I.; Garcerá, G.; Figueres, E. "A Control Scheme to Suppress Circulating Currents in Parallel-Connected Three-Phase Inverters" *Electronics* 2022, 11, 3720.